

# Unveiling the Power of Self-supervision for Multi-view Multi-human Association and Tracking

Wei Feng, *Member, IEEE*, Feifan Wang, Ruize Han, *Student Member, IEEE*, Zekun Qian, and Song Wang, *Senior Member, IEEE*

**Abstract**—Multi-view multi-human association and tracking (MvMHAT), is a new but important problem for multi-person scene video surveillance, aiming to track a group of people over time in each view, as well as to identify the same person across different views at the same time, which is different from previous MOT and multi-camera MOT tasks only considering the over-time human tracking. This way, the videos for MvMHAT require more complex annotations while containing more information for self learning. In this work, we tackle this problem with a self-supervised learning aware end-to-end network. Specifically, we propose to take advantage of the spatial-temporal self-consistency rationale by considering three properties of reflexivity, symmetry and transitivity. Besides the reflexivity property that naturally holds, we design the self-supervised learning losses based on the properties of symmetry and transitivity, for both appearance feature learning and assignment matrix optimization, to associate the multiple humans over time and across views. Furthermore, to promote the research on MvMHAT, we build two new large-scale benchmarks for the network training and testing of different algorithms. Extensive experiments on the proposed benchmarks verify the effectiveness of our method. We have released the benchmark and code to the public.

**Index Terms**—multiple object tracking, human association, multi-view cameras, self-supervised learning

## 1 INTRODUCTION

MULTIPLE object tracking (MOT), especially multiple human tracking, is a fundamental and important task in computer vision [1], [2], [3]. In this paper, we study the problem of multi-view multi-human association and tracking (MvMHAT), an extension of MOT, which aims to continuously track a group of people in each view while simultaneously identifying the same persons across multiple views at each time [4]. With MvMHAT, we can not only record the temporal trajectories of the involved humans (referred to as subjects in this paper), but also comprehensively observe the subjects' details, e.g., the human pose and behavior, by combining information from different views, which are desirable in many potential real-world applications. A typical example is video surveillance – imagine a scenario with multiple pre-installed or wearable cameras covering a scene of multiple subjects from different views, we can associate and analyze the collected videos for collaborative human activity recognition, important/abnormal person detection, etc., based on the MvMHAT results.

Compared to MOT, MvMHAT is a more challenging problem since we need to associate all the subjects appearing in different views during the tracking. The association also suffers from the unknown and large view differences, illumination differences, e.g., View #1 and View #2 in Fig. 1, and the difference of contained subjects, e.g., Views #1 and #V at Time  $t_3$ , etc. Moreover, with the *uncalibrated* multi-view cameras, e.g., wearable cameras, many existing multi-view human association methods are not applicable without the required camera relative pose as input [5], [6]. Also, the human motion feature, a core cue for human matching in

tracking, is usually inconsistent across different views and may not be effective when used for measuring the subject similarity for the cross-view association. In this case, the subject appearance representation becomes particularly important.

So far, MvMHAT is a relatively new task with a handful of studies [4], [7], [8]. Among them, most mainly study the over-time human tracking but not much in-depth study and evaluation on the cross-view human association results [5], [6], [7], [8]. Note that by focusing only on the temporal tracking in respective view but not the correspondence across different views, the advantage of the multi-view multi-human tracking is not fully exploited. A couple of recent works [4], [9] study the MvMHAT with two specific complementary views, i.e., top and horizontal views. In this paper, as shown in Fig. 1, we are interested in MvMHAT in a more general setting where (arbitrary) multiple cameras (without prior calibration) are used to observe a multi-person scene from different views.

For this purpose, we propose to develop a unified framework for the MvMHAT with arbitrary number of views. As discussed above, a key point for this problem is to learn the human appearance similarity and the association relations of the subjects among all views over time. As we know, most previous works for MOT learn an appearance model from abundant labeled data for the over-time appearance measurement. On one hand, for MvMHAT, the labor cost of annotation is greatly increased, which limits the emergence of some large-scale and high-quality datasets for network training. On the other hand, in the MvMHAT problem, we actually have various appearance information of each subject along time and across views. For example, the same person appearing in a pair of frames (views or time) should present symmetric-consistent, i.e., given two frames, if one person in frame 1 has the highest similarity with someone in frame 2, then this person in frame 2 should also be the most similar to that person in frame 1; the same person appearing in multiple frames

- W. Feng, F. Wang, R. Han (Corresponding Author) and Z. Qian are with the College of Intelligence and Computing, Tianjin University, Tianjin, 300350, China, and with the Key Research Center for Surface Inspection and Analysis of Cultural Relics, SACH, China.  
S. Wang is with the Department of Computer Science and Engineering, University of South Carolina, Columbia, SC 29208, USA.

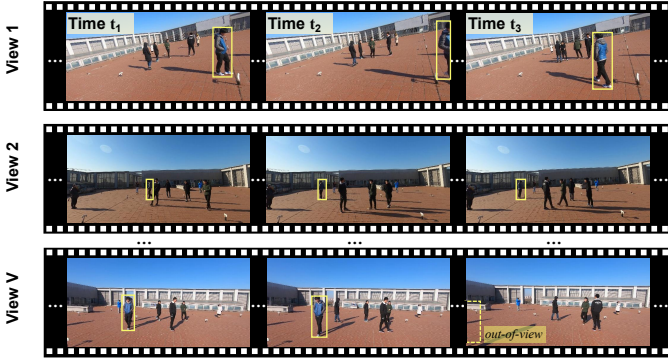


Fig. 1. An illustration of the proposed MvMHAT problem.

should also be transitive-consistent, i.e., given the matched person pairs appearing in frames 1&2, and frames 2&3, her/his matching relation between frames 1&3 should be the same as the result of associating these two matching pairs. These two observations motivate us to adopt a self-supervised learning based method to utilize the spatial-temporal human appearance consistency and association consistency for MvMHAT.

As discussed above, in this paper, we propose a self-supervised learning framework to solve the MvMHAT problem. In the training stage, our basic idea is to make use of the *spatial-temporal self-consistency* of the humans in different frames (taken from different views or time) for *both appearance feature and assignment matrix learning*. Specifically, given several videos capturing a group of people from different views, we first sample several frames from different views and time, then we apply the convolutional neural networks (CNN) to learn the embedding feature of each subject. We use the feature similarity of the subjects in each pair of frames to generate the matching matrix. We then propose a couple of symmetric-consistency (SymC) and transitive-consistency (TrsC) as pretext task to supervise the matching matrix for learning the appearance feature in the self-supervised manner. Then, we propose a spatial-temporal assignment network (STAN) to simultaneously model the over-time temporal association and the cross-view spatial association, which generates the assignment matrix considering the global structural information for MvMHAT. The STAN is also trained using the SymC and TrsC alike losses in a self-supervised way. In the inference stage, we leverage a new joint association and tracking scheme to solve the MvMHAT task.

Moreover, the current research on MvMHAT is restricted by the lack of an appropriate public dataset that can be accessed and used to train and evaluate the deep network based algorithms. In this paper, we build two new large-scale benchmarks based on several public datasets and self-collected data for the training and testing of the MvMHAT algorithm. The main contributions of this paper are:

- 1) We propose a self-supervised learning framework for MvMHAT, which in-depth excavate the potential of spatial-temporal self-consistency rationale in this problem. To the best of our knowledge, this is the first work to model such a problem following a self-supervised manner.
- 2) We propose the pairwise symmetric-consistency and triplewise transitive-consistency pretext tasks, which are guaranteed by the theoretical support and effectively used for both appearance feature and assignment matrix learning in our method. They are also modeled as differentiable loss functions, to build the end-to-end

framework for the cross-view and over-time subject association and tracking.

3) We build two new benchmarks for training and testing MvMHAT. Extensive experiments on the proposed datasets verify the rationality of our problem definition, the usefulness of the proposed benchmark, and the effectiveness of our method. We have released the benchmark to the public<sup>1</sup>.

The remainder of this paper is organized as below. Section 2 reviews the related works. Section 3 elaborates on the proposed approach in detail. Section 4 presents the benchmark used in this work. Section 5 provides the experimental results and analysis. After that, we provide a further discussion in Section 6 and a brief conclusion and future work in Section 7. This paper is a substantial extension from a preliminary conference version [10] with a number of major changes. First, we add a new spatial-temporal assignment matrix learning module (Section 3.4), which shares the self-consistency rationale for the appearance feature learning module in [10] to together form a fully self-supervised end-to-end framework. Second, a new pseudo label generation strategy with dummy nodes used for more general MvMHAT cases is introduced in Section 3.3.3. Third, we include a new dataset MMP-MvMHAT and significantly extend the experimental comparisons and analyses in Section 5. Finally, we add the discussion about the limitations and future work in Sections 6 and 7.

## 2 RELATED WORK

**MOT** is a classical problem and has many applications in video processing and analysis. The most famous framework for MOT is a tracking-by-detection scheme, in which an object detector is first applied, and the remaining task is to associate the generated detections. In this scheme, the most important issue is data association, which is mostly based on appearance similarity and motion consistency. The motion features are mainly based on linear and nonlinear motion models. The linear model assumes the target to have a linear movement with constant velocity for a period of time [11], [12], [13], which is used in most existing trackers. The nonlinear one, to some extent, can better capture the various movements and provide a more accurate motion prediction [14], [15]. Many previous works on MOT try to develop more powerful appearance feature for object association, from the hand-crafted appearance features such as color histograms [11], [16], to the recent deep network based appearance features [3], [17], [18]. This way, a key issue for such tracking-by-detection methods lies in the learning of human appearance features. More recent works also try to achieve object detection and tracking simultaneously using an end-to-end framework [19], [20], [21], [22], e.g., making the detection and tracking to complement each other [21], or excavating useful information from the low-confidence detection boxes [22]. More recently, some trackers based on graph neural networks (GNN), e.g., [23] or transformers, e.g., [24], [25], [26] are proposed and achieve the promising performance. For a more comprehensive review on MOT, we refer readers to some excellent surveys on tracking [27], [28]. Note that, the problem studied in this paper is based on the MOT technique but not focus on the study of general MOT.

**MTMCT** (Multi-Target Multi-Camera Tracking) is an extension of MOT, which aims to track and re-identify the targets (mainly for humans) in a large field, e.g., a campus, using many

1. <https://github.com/realgump/MvMHAT>

cameras installed at many sites with little or no field of view overlap. Some related works in this area [29], [30], [31], [32] focus on the inter-camera tracklets association by assuming that the within-camera tracklets in each camera are prior given or obtained by existing algorithms. This setting is not practical in a real-world application. Some other works aim to address a more realistic problem by solving both intra- and inter-camera tracking jointly [13], [33], [34], [35]. The main thought for solving such a problem is to learn more discriminative appearance features [13] or design a more exquisite optimization model [35]. Differently, we are more interested in handling multi-human association and tracking problem to comprehensively observe a crowd from different perspectives as discussed below.

**MvMHAT** and **MTMCT** both stem from MOT task. However, they are different in that the former focuses on both the *over-time human tracking* and the *cross-view association at each time among multi-view videos*, where the multiple cameras pay co-attention on an overlapped area. The latter emphasizes the *long-term human tracking and re-identification* (cross-camera association) using multiple cameras covering different areas. Two classic differences are 1) They have different problem definitions. Besides single-view intra-camera tracking, **MTMCT** also aims to handle the human re-identification, which is a ranking problem. Differently, **MvMHAT** focuses on the frame-by-frame multi-human cross-view association, which is a multi-graph matching problem. 2) They use different camera settings. **MTMCT** uses multiple cameras distributing at different sites in a large-scale area with no field-of-view (FOV) overlap. Differently, **MvMHAT** uses multi-view all-around cameras with overlapping FOVs covering the same scene.

Some early works [7], [36], [37], [38], [39], [40] similar to **MvMHAT** have studied the similar problems of tracking multiple humans using several overlapped cameras, in which the subjects commonly appear in different views at the same time. Recently, a series of works proposed by Xu et al. [8], [41], [42] propose the tracking of multiple people in a scene, e.g., a garden, using several cameras and collect new datasets for research. This series of works develop various human features for tracking, including the varied poses and human actions, etc. However, the above works mainly focus on the over-time human tracking performance but not assessing the cross-view human association results. A recent work [5] proposes to handle the multi-view human association and 3D pose estimation problem, in which a 3D pose tracking is integrated to obtain the temporal human pose. Similarly, Dong et al. [6] develop a self-supervised method for human association, which adapts the generic person appearance descriptor to the unlabeled videos by exploiting motion tracking, mutual exclusion constraints, and multi-view geometry. These couple of works both require the camera calibration, which is not practicable in this work where the camera may keep moving over time. More recently, a series of works by Han et al. [4], [9] propose to jointly solve the human association and tracking problem using two complementary views, which, however, is a specific setting and used for several application scenarios. Differently, in this paper, we focus on a more general setting where (arbitrary) multiple cameras observe a scene from different views.

Also related to our work is a study on multi-view multi-object association (matching) [43], [44], [45], [46], [47] by exploring the matching cues, including human appearance [43], [46], spatial relation [44], [47] or motions [45], all of which only focus on cross-view association but not involving the over-time tracking.

**Self-supervised Learning** is a form of unsupervised learning,

which has been widely used in many vision and multimedia computing tasks, including the image-based representation learning [48], [49] and video-level temporal coherence [50], [51], in particular, including person re-identification (re-id) [52], [53], [54] which is similar to our problem that learns the appearance similarity. The global matching based re-id features can not be directly used for MOT, which is regarded as a local association problem [55]. However, there are rare works on studying the unsupervised learning based MOT, especially for the multi-human tracking [56], [57], not to mention the **MvMHAT**. Specifically, as one branch of unsupervised learning, self-supervised learning aims to construct the pretext tasks, commonly obtained by the acknowledged prior or self-constraint, to learn the network from unlabeled data. In this paper, we aim to unveil the power of self-supervised learning for data association in **MvMHAT**.

## 3 THE METHOD

### 3.1 Problem Formulation

Given  $V$  synchronized video sequences taken from different views, we aim to achieve the multi-view multi-human association and tracking (**MvMHAT**), which collaboratively tracks all subjects in all videos as well as identifies all the same person appearing in different views. Specifically, we assume that the subjects have been detected in each frame in advance: the subjects are represented as bounding boxes in each view  $v$  at each time  $t$ . For each person in each view, **MvMHAT** aims to connect the subjects to form the single-view trajectory. Besides, **MvMHAT** also identifies each trajectory belonging to the same person in all views.

In this work, we formulate the above collaborative tracking, i.e., **MvMHAT**, as a spatial-temporal subject association problem. On one hand, the temporal (over-time) association can be regarded as a single-view multiple object tracking (MOT) problem. Similar with most MOT approach, the goal is to solve the association matrix between the tracklets  $\mathcal{T}_{t-1}$  until frame  $t-1$  in view  $v$ , and all the detections  $\mathcal{B}_t^v = \{B_i | i = 1, 2, \dots, N_t^v\}$  on frame  $t$ . Thus the association matrix is represented as  $\mathbf{A}_t^v \in \mathbb{R}^{M_{t-1} \times N_t^v}$ , where  $M_{t-1}$  and  $N_t^v$  denote the number of trajectories  $\mathcal{T}_{t-1}$  and subjects  $\mathcal{B}_t^v$ , respectively. On the other hand, the spatial (cross-view) association is a multi-view subject matching problem. At each time  $t$ , we establish the association relation between different views. Taking a pair of views  $v$  and  $u$  as an example, the cross-view subject association between  $\mathcal{B}_t^v$  and  $\mathcal{B}_t^u$  can be represented as a matching matrix  $\mathbf{A}^{v,u} \in \mathbb{R}^{N_t^v \times N_t^u}$ , where  $N_t^u$  denotes the number of subjects in  $\mathcal{B}_t^u$ .

### 3.2 Spatial-Temporal Self-Consistency

As shown in Fig. 3, the multi-view video sequences provide the all-around and time-varying appearance of the subjects in the scene. The same person appearing in pairwise views or points of time presents symmetric-consistency in Fig. 3(a). They also show transitive-consistency among multiple views and time in Fig. 3(b). This inspires us to unveil self-supervised power for establishing the over-time and cross-view subject similarity. In the following, we elaborate on these consistencies and develop a self-supervised learning network for spatial-temporal subject association.

The basic idea of the proposed self-supervised learning strategy is the Spatial-Temporal Self-Consistency contained in the **MvMHAT** problem. We consider two pretext tasks to construct the self-supervised loss. First, the same person appearing in a

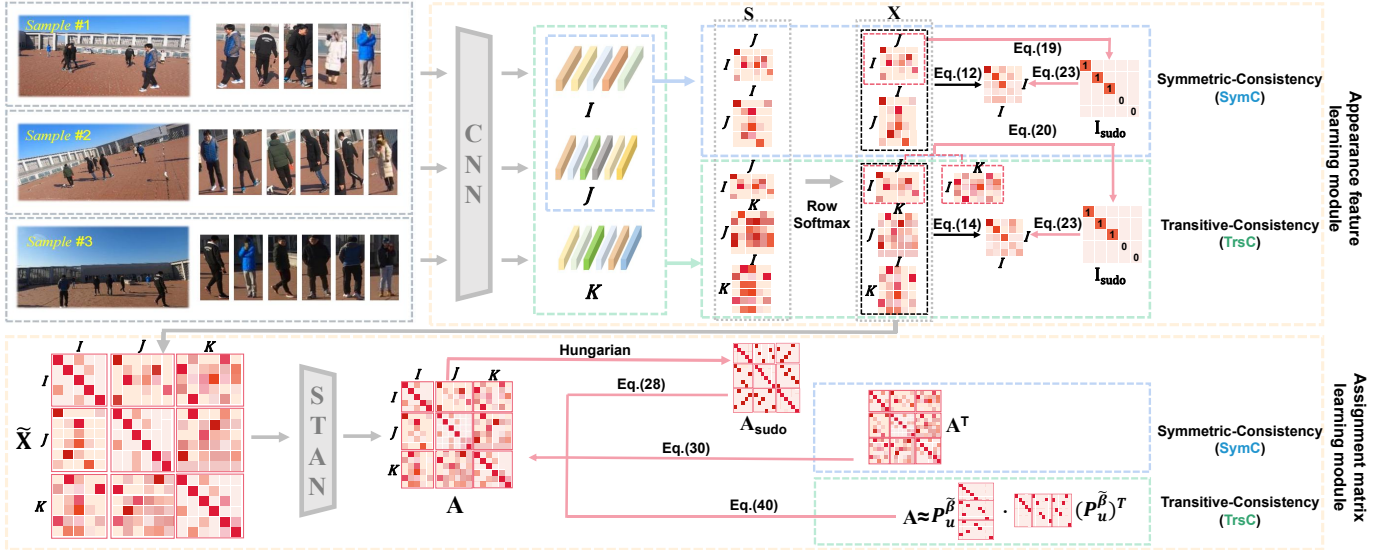


Fig. 2. Overall framework of the proposed method, where we take three frames as an example. Specifically, we use the frames from different views and time and their human detection results as an input batch in the training stage. The framework consists of two parts: appearance feature learning module and assignment matrix learning module, for each of which we use the symmetric-consistency and transitive-consistency discussed in Section 3.2 to construct the self-supervised loss for training.

pair of frames from different views or different time should be consistent. As shown in Fig. 3(a), for a subject #A in Frame #1, if the subject #A' in another Frame #2 has the highest similarity with #A among all subjects; the subject #A should be the most similar with #A' among all subjects in Frame #1, i.e., the symmetric-consistency property. Second, as shown in Fig. 3(b), the subject has transitive consistency among multiple views and different time. For example, if subject #A in Frame #1 is identity-consistent with #A' in Frame #2 and the subject #A'' in Frame #3, then the subjects #A' and #A'' should be the same subject, i.e., the transitive-consistency property.

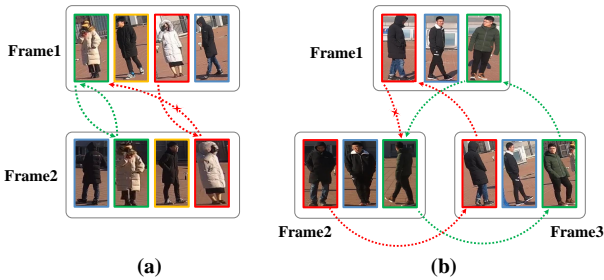


Fig. 3. An illustration of symmetric and transitive consistency rationale.

From the above observation, we obtain the following mathematical formalization: let  $\mathcal{B} = \cup_{v=1 \dots V} \mathcal{B}_v^v$ , we define a subject consistency relation  $\mathcal{R} = \{(B, B') | B, B' \in \mathcal{B}, B \text{ and } B' \text{ denote the same person}\} \subseteq \mathcal{B} \times \mathcal{B}$ , where  $\times$  represents Cartesian product. Clearly  $\mathcal{R}$  satisfies the following properties

- (1) **Reflexivity:**  $(B, B) \in \mathcal{R}, \quad \forall B \in \mathcal{B}$  (1)
- (2) **Symmetry:**  $(B, B') \in \mathcal{R} \Rightarrow (B', B) \in \mathcal{R}, \quad \forall (B, B') \in \mathcal{R}$  (2)
- (3) **Transitivity:**  $(B, B') \in \mathcal{R}, (B', B'') \in \mathcal{R} \Rightarrow (B, B'') \in \mathcal{R},$   
 $\forall (B, B'), (B', B'') \in \mathcal{R}$  (3)

We simplify the subject set in view  $v$  at time  $t$ , i.e.,  $\mathcal{B}_t^v \subseteq \mathcal{B}$ , as

$\mathcal{B}_i$ . We first assume that all  $\mathcal{B}_i$  share the same set of subjects. We know this is difficult to hold in reality, and we will consider the more general case later. We then denote the subject consistency relation between arbitrary set pair  $(\mathcal{B}_i, \mathcal{B}_j)$  as  $\varphi_{\mathcal{B}_i \mathcal{B}_j} \subseteq \mathcal{R}$ , i.e.,  $\varphi_{\mathcal{B}_i \mathcal{B}_j} = \{(B, B') | B \in \mathcal{B}_i, B' \in \mathcal{B}_j, B \text{ and } B' \text{ denote the same person}\}$ . Then from Eqs. (1-3) we can get

$$(1) \text{ Reflexivity: } \varphi_{\mathcal{B}_i \mathcal{B}_i} = id_{\mathcal{B}_i} \quad (4)$$

$$(2) \text{ Symmetry: } \varphi_{\mathcal{B}_i \mathcal{B}_j} \triangleleft \varphi_{\mathcal{B}_j \mathcal{B}_i} = id_{\mathcal{B}_i} \quad (5)$$

$$(3) \text{ Transitivity: } \varphi_{\mathcal{B}_i \mathcal{B}_j} \triangleleft \varphi_{\mathcal{B}_j \mathcal{B}_k} \triangleleft \varphi_{\mathcal{B}_k \mathcal{B}_i} = id_{\mathcal{B}_i} \quad (6)$$

where  $\triangleleft$  denotes the left outer join operation to connect multiple  $\varphi$ , and  $id_{\mathcal{B}_i}$  is the identity mapping of  $\mathcal{B}_i$ . This is to say the properties of reflexivity, symmetry and transitivity also maintain among the consistency relations  $\varphi$ . In the following, we propose to use above self-consistency properties for subject feature learning in Section 3.3 and assignment matrix solving in Section 3.4.

### 3.3 Self-Consistency for Appearance Feature Learning

#### 3.3.1 Feature Extraction

The overall framework is shown in Fig. 2, which takes the video sequence without annotation as input and learns the subject similarity used for association in a self-supervised manner. Specifically, given an arbitrary video frame  $i$ , we first apply a human detector to obtain all the subjects  $\mathcal{B}_i$  in this frame. With the detected subjects, we apply the feature extraction network, denoted as  $\Phi$ , to get the feature representation for all subjects  $\mathbf{E}_i = \Phi(\mathcal{B}_i)$ , by which we get  $\mathbf{E}_i \in \mathbb{R}^{N_i \times D}$ , here  $N_i$  denotes the number of subjects in frame  $i$ , and  $D$  denotes the dimension of feature for each subject. With the extracted features on each frame, we can then define the subject similarity and association across views or over time.

**Spatial-temporal association.** Given a pair of frames  $i, j$  from different views or time, the subject similarity matrix among all subjects in the respective frame can be calculated by

$$\mathbf{S}_{ij} = \mathbf{E}_i \cdot (\mathbf{E}_j)^T \in \mathbb{R}^{N_i \times N_j}, \quad (7)$$

whose value at  $r$ -th row and  $c$ -th column, i.e.,  $\mathbf{S}_{i,j}(r, c)$  represents the similarity between  $r$ -th subject in  $\mathcal{B}_i$  and  $c$ -th subject in  $\mathcal{B}_j$ . We then consider obtaining the pairwise matching matrix  $\mathbf{X}_{ij} \in [0, 1]^{N_i \times N_j}$  based on the above similarity matrix. For clarity, we provisionally simplify the similarity and matching matrices  $\mathbf{S}_{ij}$  and  $\mathbf{X}_{ij}$  as  $\mathbf{S}$  and  $\mathbf{X}$ . We use a temperature-adaptive *softmax* operation  $f$  [58] to compute the matching matrix as

$$\mathbf{X}(r, c) = f_{r,c}(\mathbf{S}) = \frac{\exp(\tau \mathbf{S}(r, c))}{\sum_{c'=1}^C \exp(\tau \mathbf{S}(r, c'))}, \quad (8)$$

where  $r, c$  denote the index of row and column in  $\mathbf{S}$  and  $C$  is the number of columns for  $\mathbf{S}$ . That is we apply the *softmax* operation on each row of the matrix  $\mathbf{S}$  and get  $\mathbf{X}$  with same size as  $\mathbf{S}$  taking values in  $[0, 1]$ , as shown in Fig. 2. In Eq. (8), we use the *softmax* with a adjustable value  $\tau$  as the adaptive temperature

$$\tau = \frac{1}{\epsilon} \log \left[ \frac{\delta(C-1) + 1}{1 - \delta} \right], \quad (9)$$

to control the soften ability of the function, where  $\epsilon$  and  $\delta$  are two pre-set parameters.

So far, we get the predicted matching matrix  $\mathbf{X}$ . If we have the annotated data with a human identification label, the network can be trained with the supervision of ground-truth  $\mathbf{X}$ . In this paper, we aim to explore the spatial-temporal self-consistency for learning the network without manual labels.

### 3.3.2 Self-Consistency Learning

**Symmetric-Consistency (SymC).** Given the similarity matrix between the subjects within two sets  $\mathcal{I}$  and  $\mathcal{J}$  (including the cross-view or over-time cases) as defined in Eq. (7), which we denoted as  $\mathbf{S}_{ij} \in \mathbb{R}^{|\mathcal{I}| \times |\mathcal{J}|}$ , where  $|\cdot|$  denotes the number of elements in the set. We apply the *softmax* operation on the similarity matrix  $\mathbf{S}$  to get the matching matrix defined in Eq. (8) as

$$\mathbf{X}_{ij} = f(\mathbf{S}_{ij}) \in \mathbb{R}^{|\mathcal{I}| \times |\mathcal{J}|}. \quad (10)$$

The matching matrix  $\mathbf{X}_{ij}$  can be regarded as a mapping (matching relation) from  $\mathcal{I}$  to  $\mathcal{J}$ , i.e.,  $\mathcal{X}_{ij} : \mathcal{I} \mapsto \mathcal{J}$ . Specifically, the row sum in  $\mathbf{X}$  is equal to 1, and we can find the maximum in each row of  $\mathbf{X}$  to seek the matched subject of someone in  $\mathcal{I}$  from  $\mathcal{J}$ . Similarly, we get the mapping from  $\mathcal{J}$  to  $\mathcal{I}$  as

$$\mathbf{X}_{ji} = f(\mathbf{S}_{ij}^T) \in \mathbb{R}^{|\mathcal{J}| \times |\mathcal{I}|}. \quad (11)$$

According to the ‘symmetry’ property in Eq. (5), we calculate the *symmetric-similarity matrix*

$$\mathbf{I}_S = \mathbf{X}_{ij} \cdot \mathbf{X}_{ji} \in \mathbb{R}^{|\mathcal{I}| \times |\mathcal{I}|}, \quad (12)$$

where  $\mathbf{I}_S$  can be regarded as the mapping:  $\mathcal{I} \mapsto \mathcal{J} \mapsto \mathcal{I}$ . Ideally, if the subjects in  $\mathcal{I}$  and  $\mathcal{J}$  are same, the result  $\mathbf{I}_{ideal}$  (i.e., the ideal approximation matrix (ground-truth result) of  $\mathbf{I}_S$ ) should be an identity matrix. This way, we can calculate the loss between predicted  $\mathbf{I}_S$  and the identity matrix. As discussed above, this assumption is not always satisfied due to the occluded or out-of-view subjects over time and the field-of-view difference across views, which causes the all-zero row appearing in  $\mathbf{I}_{ideal}$ . Therefore, we can not always compel the result  $\mathbf{I}_S$  to approximate the identity matrix and have to apply more deliberate supervision on it, which will be discussed later.

**Transitive-Consistency (TrsC).** Besides the pairwise symmetric similarity, we also consider the triplewise transitive similarity. Given the similarity matrix  $\mathbf{S}_{ij}$  between two sets  $\mathcal{I}$  and

$\mathcal{J}$ ,  $\mathbf{S}_{jk}$  between  $\mathcal{J}$  and  $\mathcal{K}$ , and  $\mathbf{S}_{ki}$  between  $\mathcal{K}$  and  $\mathcal{I}$ , we also consider the transitive similarity within this triplet, i.e.,  $\mathcal{I}, \mathcal{J}$  and  $\mathcal{K}$ . We first compute their corresponding matching matrix as

$$\begin{aligned} \mathbf{X}_{ij} &= f(\mathbf{S}_{ij}) \in \mathbb{R}^{|\mathcal{I}| \times |\mathcal{J}|}, & \mathbf{X}_{jk} &= f(\mathbf{S}_{jk}) \in \mathbb{R}^{|\mathcal{J}| \times |\mathcal{K}|}, \\ \mathbf{X}_{ki} &= f(\mathbf{S}_{ki}) \in \mathbb{R}^{|\mathcal{K}| \times |\mathcal{I}|}, & (i \neq j \neq k) \end{aligned} \quad (13)$$

The result  $\mathbf{X}_{ij}$ ,  $\mathbf{X}_{jk}$  and  $\mathbf{X}_{ki}$  represent the mapping  $\mathcal{I} \mapsto \mathcal{J}$ ,  $\mathcal{J} \mapsto \mathcal{K}$  and  $\mathcal{K} \mapsto \mathcal{I}$  respectively. Then, according to the ‘transitivity’ property in Eq. (6), we calculate the *transitive-similarity matrix* as

$$\mathbf{I}_T = \mathbf{X}_{ij} \cdot \mathbf{X}_{jk} \cdot \mathbf{X}_{ki} \in \mathbb{R}^{|\mathcal{I}| \times |\mathcal{I}|}, \quad (14)$$

where  $\mathbf{I}_T$  can be regarded as the mapping:  $\mathcal{I} \mapsto \mathcal{J} \mapsto \mathcal{K} \mapsto \mathcal{I}$ . Similar with the matrix  $\mathbf{I}_S$  defined in Eq. (12), we need to apply an appropriate supervision on both  $\mathbf{I}_S$  and  $\mathbf{I}_T$ , which will be elaborated in detail in Section 3.3.3.

**Generalized TrsC.** Up to now, we have present the pairwise symmetric similarity, the triplewise transitive similarity constraints. Actually, the transitive-consistency should be satisfied in the more general cases where more views or time are involved. In the following, we discuss the generalization of the proposed self-consistency constraints.

As discussed in Section 3.2, we first assume all the frames share the same set of subjects. This way, given any  $n(n \geq 3)$  frames, the transitive-consistency among  $n$  frames requires

$$\varphi_{\mathcal{B}_1 \mathcal{B}_n} = \varphi_{\mathcal{B}_1 \mathcal{B}_2} \triangleleft \cdots \triangleleft \varphi_{\mathcal{B}_{n-2} \mathcal{B}_{n-1}} \triangleleft \varphi_{\mathcal{B}_{n-1} \mathcal{B}_n}. \quad (15)$$

The above combined mapping can be derived by the proposed pairwise and triplewise mapping.

**Inference.** Equation (15) can be guaranteed by

$$\varphi_{\mathcal{B}_i \mathcal{B}_k} = \varphi_{\mathcal{B}_i \mathcal{B}_j} \triangleleft \varphi_{\mathcal{B}_j \mathcal{B}_k}, \quad \text{for } \forall \mathcal{B}_i, \mathcal{B}_j, \mathcal{B}_k \subseteq \mathcal{B}, \quad (16)$$

from which we discuss the situations in three cases:

- (i)  $i = k = j$ : it is equivalent to the Reflexivity in Eq. (4).
- (ii)  $i = k \neq j$ : it is equivalent to the Symmetry in Eq. (5).
- (iii)  $i \neq k \neq j$ : it is equivalent to the Transitivity in Eq. (6).

Note that, these three cases cover all the scenarios. The reflexivity condition naturally holds in our problem because the same person in the same frame has the same feature vector. This way, we only consider the conditions in (ii) and (iii), for which we use the doubly stochastic matching matrix  $\mathbf{X}_{ij}$  to represent the consistency relation  $\varphi$ . We get

$$\text{(Symmetric-Similarity)} \quad \mathbf{X}_{ij} \cdot \mathbf{X}_{ji} = \mathbf{I} \quad (17)$$

$$\text{(Transitive-Similarity)} \quad \mathbf{X}_{ij} \cdot \mathbf{X}_{jk} \cdot \mathbf{X}_{ki} = \mathbf{I} \quad (18)$$

where  $\mathbf{I}$  is the identity matrix. This way, the proposed method with self-supervision from symmetric-similarity Eq. (12) and transitive-similarity Eq. (14), can be regarded as the self-consistency constraints for the matching relations among arbitrary  $n$  frames. ■

In the above inference, we assume all the frames share the same set of subjects. Actually, this is not always satisfied in our problem. Therefore, we only assume  $\mathbf{X}$  is the row stochastic matrix (sum of each row is 1). We also consider the dummy nodes and a relaxing strategy to construct the loss function for the supervision of  $\mathbf{I}$ , which is presented as below.

### 3.3.3 Self-supervised Loss for Feature Consistency

Next, we uniformly denote the matrix  $\mathbf{I}_S$  in Eq. (12) and  $\mathbf{I}_T$  in Eq. (14) as  $\mathbf{I}$  provisionally. Its ideal approximation matrix

$\mathbf{I}_{\text{ideal}}$  have the property that their diagonal elements are 1 or 0, while other elements are all 0. Note that, the element of 0 in the diagonal denotes that the subject is missing (due to the occlusion or out of view, etc) in one view. However, for the self-supervised method, we can not obtain the ideal approximation matrix  $\mathbf{I}_{\text{ideal}}$  for supervision. A simple method is to use a diagonal identity matrix to supervise  $\mathbf{I}$  with a relaxation [10], which ignores the case of missing subjects. Differently, in this work, we handle this problem by constructing a dummy nodes integrated pseudo matrix label to self-supervise  $\mathbf{I}$ .

**Pseudo matrix label with dummy nodes.** First, let's think about the symmetric-consistency. Given two sets  $\mathcal{I}$  and  $\mathcal{J}$ , if a certain person in set  $\mathcal{I}$  also appear in set  $\mathcal{J}$ , then after the mapping from  $\mathcal{I} \mapsto \mathcal{J} \mapsto \mathcal{I}$ , the diagonal element value of the corresponding row of this person in  $\mathbf{I}_{\text{ideal}}$  matrix should be 1; otherwise 0. This way, we construct the pseudo matrix label as

$$\mathbf{I}_{\text{sudo}}^{\text{S}}(r, r) = \begin{cases} 1, & \max_c \mathbf{X}_{ij}(r, c) > M \\ 0, & \text{otherwise} \end{cases} \quad (19)$$

where  $\mathbf{X}_{ij}$  is obtained by the row softmax operation on  $\mathbf{S}_{ij}$  matrix as defined above. For each row in  $\mathbf{X}_{ij}$  (i.e. each person in set  $\mathcal{I}$ ) represents the matching scores with each person in set  $\mathcal{J}$ . Therefore, for each row in  $\mathbf{X}_{ij}$ , if the maximum value of the row is greater than the matching threshold  $M$ , it is considered that the person also appears in the set  $\mathcal{J}$ , and we can conclude that the diagonal element value of this row in  $\mathbf{I}_{\text{sudo}}$  is 1; otherwise 0.

For the the transitive-consistency, given three sets  $\mathcal{I}$ ,  $\mathcal{J}$  and  $\mathcal{K}$ , if a certain person in set  $\mathcal{I}$  also appear in set  $\mathcal{J}$  and  $\mathcal{K}$ , the diagonal element value of the corresponding row for this person in  $\mathbf{I}_{\text{ideal}}$  matrix should be 1; otherwise 0. Similarly with Eq. (19), we construct the pseudo matrix label as

$$\mathbf{I}_{\text{sudo}}^{\text{T}}(r, r) = \begin{cases} 1, & \max_{c_1} \mathbf{X}_{ij}(r, c_1) > M \wedge \max_{c_2} \mathbf{X}_{ik}(r, c_2) > M \\ 0, & \text{otherwise} \end{cases} \quad (20)$$

where we use  $\mathbf{X}_{ij}$  and  $\mathbf{X}_{ik}$  for judgement.

**Loss function design.** We also uniformly denote the pseudo matrices  $\mathbf{I}_{\text{sudo}}^{\text{S}}$  and  $\mathbf{I}_{\text{sudo}}^{\text{T}}$  as  $\mathbf{I}_{\text{sudo}}$ . Here we do not directly use  $\mathbf{I}_{\text{sudo}}$  matrix to compute the difference with  $\mathbf{I}$  as loss. This is because  $\mathbf{X}_{ij}$  matrix is obtained by row softmax, it is impossible to have a row with all 0 values, as discussed in [10], [59]. So, the off-diagonal elements values in  $\mathbf{I}$  matrix, obtained by multiplication of  $\mathbf{X}_{ij}$ , are also not 0, while the off-diagonal elements values in  $\mathbf{I}_{\text{sudo}}$  are all 0. The direct difference between them as loss might bring in additional error. This way, we design the loss function according to the characteristics of  $\mathbf{I}_{\text{sudo}}$ .

1) When the diagonal element of a row in  $\mathbf{I}_{\text{sudo}}$  is 1. We can easily find that its characteristic is that the value of the diagonal element is greater than its off-diagonal elements. So the diagonal element of  $\mathbf{I}$  should be greater than the others in this row. With this constraint, we apply the loss function as below

$$L_1(\mathbf{I}_r) = \text{relu}(\max_{c \neq r} \mathbf{I}(r, c) - \mathbf{I}(r, r) + m_1) \quad (21)$$

where  $r, c$  denote the indices of row and column in  $\mathbf{I}$ , i.e.,  $\mathbf{I}_r$  denotes the  $r$ -th row of matrix  $\mathbf{I}$ . Specifically, for each row  $r$ , if the off-diagonal elements  $\mathbf{I}(r, c)$  with  $c \neq r$  are greater than the corresponding diagonal element  $\mathbf{I}(r, r)$ , the loss will increase [59]. We only use the maximum off-diagonal element  $\max_{c \neq r} \mathbf{I}(r, c)$  in each row to punish the hardest negative sample. The margin

$m_1 \geq 0$  is a pre-set parameter, which controls the punishment scope for the gap between  $\mathbf{I}(r, c)$  and  $\mathbf{I}(r, r)$ . In other word, the loss will take effect iff  $\mathbf{I}(r, r) - \max_{c \neq r} \mathbf{I}(r, c) \leq m_1$ . This setting expects the diagonal element to be greater than the other elements with a margin  $m_1$ .

2) When the diagonal element of a row in  $\mathbf{I}_{\text{sudo}}$  is 0. We can find that its characteristic is that the value of the diagonal element is close to the values of the off-diagonal elements. Following the above idea, we define the following loss

$$L_2(\mathbf{I}_r) = \frac{1}{2} (\text{relu}(\max_{c \neq r} \mathbf{I}(r, c) - \mathbf{I}(r, r) - m_2) + \text{relu}(\mathbf{I}(r, r) - \min_{c \neq r} \mathbf{I}(r, c) - m_2)). \quad (22)$$

The margin  $m_2 \geq 0$  is also a pre-set parameter, which controls the punishment scope for the gap between  $\mathbf{I}(r, c)$  and  $\mathbf{I}(r, r)$ . Here we want to have  $|\mathbf{I}(r, c) - \mathbf{I}(r, r)| \leq m_2, \forall c \neq r$ . When this condition isn't satisfied, we penalize both the upper (max) and lower (min) bounds of it. Therefore the loss function of  $\mathbf{I}$  is defined by combining the above two cases as

$$L(\mathbf{I}) = \sum_{r=1}^{|\mathcal{I}|} \mathbf{I}_{\text{sudo}}(r, r) \cdot L_1(\mathbf{I}_r) + (1 - \mathbf{I}_{\text{sudo}}(r, r)) \cdot L_2(\mathbf{I}_r). \quad (23)$$

Finally, we define the SymC loss

$$\mathcal{L}_{\text{Sym}}^{\text{A}} = L(\mathbf{I}_{\text{S}}) + L(\mathbf{I}_{\text{S}}^{\text{T}}), \quad (24)$$

where  $L(\mathbf{I}_{\text{S}})$  and  $L(\mathbf{I}_{\text{S}}^{\text{T}})$  compels  $\mathbf{I}_{\text{S}}$  to satisfy above constraints for all rows and columns, respectively. Similarly, we get the TrsC loss

$$\mathcal{L}_{\text{Trs}}^{\text{A}} = L(\mathbf{I}_{\text{T}}) + L(\mathbf{I}_{\text{T}}^{\text{T}}). \quad (25)$$

### 3.4 Self-Consistency for Assignment Matrix Learning

In the above section, we have leveraged the self-consistency to construct the self-supervised loss for feature extraction. To handle the MvMHAT task, we aim to obtain the spatial-temporal subject assignment matrix involving multiple time and views. This way, in this section, we aim to further explore the global structure information in solving the assignment matrix, for which we also leverage the self-consistency properties as discussed in Section 3.2, and design the corresponding constraints as self-supervised losses in our framework.

#### 3.4.1 Spatial-Temporal Global Assignment

**Spatial-temporal affinity matrix generation.** From the above section, we can get the matching matrix  $\mathbf{X}_{ij}$ , which is obtained by the softmax operation through the feature similarity between the subjects in a pair of frames  $i, j$ . In the inference stage, we can use  $\mathbf{X}_{ij}$  to get the subject association results directly. However, it does not consider the information of the subjects in multiple views and multiple time. For MvMHAT task, it is not a pairwise association problem, but a spatial-temporal jointly optimized subject association problem. So the global information among multiple views and time is important and can help to get more reliable association. This way, we consider to use the matching matrix from multiple time and all views to generate the a global assignment matrix. Here we take arbitrary two points of time, i.e., time  $t$  and  $s$ , and all  $V$  views, and concatenate the subjects from them in the following order

$$\tilde{\mathbf{B}} = \mathcal{B}_t^1 \cup \dots \cup \mathcal{B}_t^V \cup \mathcal{B}_s^1 \cup \dots \cup \mathcal{B}_s^V. \quad (26)$$

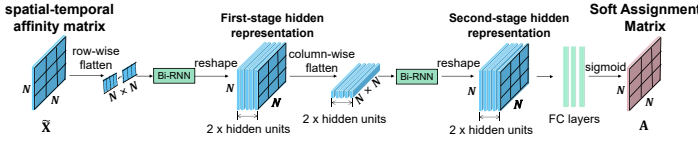


Fig. 4. An illustration of the structure of STAN.

Like before, we use feature extraction network to extract all subject feature in  $\tilde{\mathbf{B}}$  and get  $\tilde{\mathbf{E}} = \Phi(\tilde{\mathbf{B}})$ . We then calculate similarity matrix  $\tilde{\mathbf{S}} = \tilde{\mathbf{E}} \cdot \tilde{\mathbf{E}}^T$ . We first split the rows and columns of the  $\tilde{\mathbf{S}}$  according to the time and view which the subject belongs to, and then use Eq. (8) to calculate the matching matrix. This way, we can get the spatial-temporal affinity matrix  $\tilde{\mathbf{X}}$  as

$$\tilde{\mathbf{X}} = \begin{pmatrix} \mathbf{X}_{t,t}^{1,1} & \cdots & \mathbf{X}_{t,t}^{1,V} & \mathbf{X}_{t,s}^{1,1} & \cdots & \mathbf{X}_{t,s}^{1,V} \\ \vdots & \ddots & \vdots & \vdots & \ddots & \vdots \\ \mathbf{X}_{t,t}^{V,1} & \cdots & \mathbf{X}_{t,t}^{V,V} & \mathbf{X}_{t,s}^{V,1} & \cdots & \mathbf{X}_{t,s}^{V,V} \\ \mathbf{X}_{s,t}^{1,1} & \cdots & \mathbf{X}_{s,t}^{1,V} & \mathbf{X}_{s,s}^{1,1} & \cdots & \mathbf{X}_{s,s}^{1,V} \\ \vdots & \ddots & \vdots & \vdots & \ddots & \vdots \\ \mathbf{X}_{s,t}^{V,1} & \cdots & \mathbf{X}_{s,t}^{V,V} & \mathbf{X}_{s,s}^{V,1} & \cdots & \mathbf{X}_{s,s}^{V,V} \end{pmatrix} \in \mathbb{R}^{|\tilde{\mathcal{B}}| \times |\tilde{\mathcal{B}}|}, \quad (27)$$

where  $\mathbf{X}_{t,s}^{u,v}$  represents the matching matrix generated by the two sets  $\mathcal{B}_t^u$  and  $\mathcal{B}_s^v$ .

**Spatial-temporal assignment network.** To build an end-to-end framework to achieve assignment optimization from the input  $\tilde{\mathbf{X}}$ , we develop a deep neural network namely STAN (spatial-temporal assignment network) to get the final assignment matrix considering the global structure. We require STAN to meet two conditions: 1) The network should be able to handle the inputs of different sizes, since the dimension of the input matrix  $\tilde{\mathbf{X}}$  is determined by  $\tilde{\mathcal{B}}$ , whose size is always changing; 2) The network must have a global receptive field for the input matrix, since the output assignment matrix should satisfy the global optimization including over-time and cross-view assignment.

Inspired by previous work [18], we use bi-directional RNN network architecture to develop the STAN, which takes the affinity matrix  $\tilde{\mathbf{X}}$  calculated above as input. As shown in Fig. 4, the input affinity matrix  $\tilde{\mathbf{X}}$  is first reshaped as a 1D vector according to the row-wise order flatten and fed into a BiRNN. Next, the output of the BiRNN is then reshaped as the 2D matrix according to the column-wise order flatten and fed into another BiRNN. Later, we apply the network composed of three FC (fully-connected) layers and a Sigmoid function to obtain the final assignment matrix  $\mathbf{A}$ .

### 3.4.2 Self-supervised Loss

We aim to design the self-supervised loss function to train STAN. Specifically, the self-supervised loss is constructed from two aspects: 1) automatically generates pseudo label from each pair of frames that provides the basic assignment results, 2) auxiliary loss to constrain the network to include the global spatial-temporal structural information.

**Pseudo label loss.** We first consider the pseudo label by processing each sub-matrix  $\mathbf{X}_{t,s}^{u,v}$  in Eq. (27) individually to obtain a binary pseudo-label matrix. Specifically, for each  $\mathbf{X}_{t,s}^{u,v}$ , we use the Hungarian algorithm with matching threshold  $M$  to get the binary matrix as the one-to-one assignment result. We concatenate the corresponding binary matrix in the order of  $\tilde{\mathbf{X}}$  to

get the pseudo label  $\mathbf{A}_{\text{sudo}}$ . Considering the positive and negative samples in  $\mathbf{A}_{\text{sudo}}$  are unbalanced, we use the focal loss [60]

$$\mathcal{L}_{\text{Pse}}^M = \begin{cases} -\alpha(1 - a_{rc})^\gamma \log(a_{rc}) & , \text{if } \bar{a}_{rc} = 1 \\ -(1 - \alpha)(a_{rc})^\gamma \log(1 - a_{rc}) & , \text{if } \bar{a}_{rc} = 0 \end{cases} \quad (28)$$

where  $a_{rc}$ ,  $\bar{a}_{rc}$  represent the elements values of position  $(r, c)$  in  $\mathbf{A}$  and  $\mathbf{A}_{\text{sudo}}$ , respectively.  $\alpha$ ,  $\gamma$  are two pre-defined parameters.

**Symmetric-Consistency (SymC) loss.** Note that, the above pseudo label is obtained from each pairwise matching without considering any global structural constraint of the multiple time and views, which is considered in the following. We borrow the basic idea of symmetric-consistency in Eq. (2) in Section 3.2. Given sets  $\mathcal{I}$  and  $\mathcal{J}$ , if a person in  $\mathcal{I}$  has the highest similarity with someone in  $\mathcal{J}$ , then this person in  $\mathcal{J}$  should also be the most similar to that person in  $\mathcal{I}$ . Then we have

$$\mathbf{A}_{ij} = \mathbf{A}_{ji}^T, \quad \forall \mathcal{B}_i, \mathcal{B}_j \subseteq \tilde{\mathcal{B}}, \quad (29)$$

where  $\mathbf{A}_{ij}$  and  $\mathbf{A}_{ji}$  sub-matrices are in symmetrical positions in  $\mathbf{A}$ , so Eq. (29) is equivalent to  $\mathbf{A} = \mathbf{A}^T$ . Then we define the SymC loss for assignment matrix learning as

$$\mathcal{L}_{\text{Sym}}^M = \|\mathbf{A} - \mathbf{A}^T\|_2. \quad (30)$$

**Discussion.** The above constraint in Eq. (29) has not been guaranteed by the pseudo label loss in Eq. (28). This is because  $\mathbf{X}_{ij}$  matrix is obtained by row softmax from  $\mathbf{S}_{ij}$ , while the  $\mathbf{X}_{ji}$  matrix is obtained by column softmax from  $\mathbf{S}_{ji}$  with a matrix transpose, so  $\mathbf{X}_{ij}$  is not equal to  $\mathbf{X}_{ji}^T$ . Thus through the Hungarian algorithm,  $\mathbf{A}_{ij}$  is not necessarily equal to  $\mathbf{A}_{ji}^T$ . Therefore, we add the SymC loss in Eq. (30) as the constraint.

**Transitive-Consistency (TrsC) loss.** Inspired by the idea of transitive-consistency in Section 3.2, given multiple sets  $n$  ( $n \geq 3$ ), the same person appearing in these sets should be associated as a closed loop. In this section, we design the transitive-consistency loss to constrain the assignment matrix to satisfy this condition.

For this purpose, we introduce a set  $\mathcal{U}$ , which contains all the subjects with different identities in  $\tilde{\mathcal{B}}$  (i.e., the subjects from different frames but representing the same person denote the same element in  $\mathcal{U}$ ). Then we construct a row-concatenation permutation matrix (i.e., the binary assignment matrix between the elements in two sets) from  $\tilde{\mathcal{B}}$  to  $\mathcal{U}$ , i.e.,  $\mathbf{P}_{\mathcal{U}}^{\tilde{\mathcal{B}}} \in \mathbb{R}^{|\tilde{\mathcal{B}}| \times |\mathcal{U}|}$ . We clarify that if

$$\mathbf{A} = \mathbf{P}_{\mathcal{U}}^{\tilde{\mathcal{B}}} \cdot (\mathbf{P}_{\mathcal{U}}^{\tilde{\mathcal{B}}})^T \quad (31)$$

is achieved, the association result of  $\mathbf{A}$  satisfies the transitive consistency. The proof is as following.

**Inference.** When there is a row-concatenation permutation matrix from  $\tilde{\mathcal{B}}$  to  $\mathcal{U}$ , for  $\forall \mathcal{B}_i \subseteq \tilde{\mathcal{B}}$  there is also a (injective) mapping to  $\mathcal{U}$  (represented by the permutation matrix  $\mathbf{P}_{\mathcal{U}}^{\mathcal{B}_i}$ ), so we can also get an injective consistency relation from  $\mathcal{U}$  to  $\mathcal{B}_i$ , i.e.  $\varphi_{\mathcal{U}\mathcal{B}_i}$ . Since  $\mathcal{U}$  is the universal set of all appearing subjects and  $\mathcal{B}_i \mapsto \mathcal{U}$  is an injective mapping, we can get

$$\varphi_{\mathcal{B}_i\mathcal{B}_j} = \varphi_{\mathcal{B}_i\mathcal{U}} \triangleleft \varphi_{\mathcal{U}\mathcal{B}_j}, \quad \forall \mathcal{B}_i, \mathcal{B}_j \subseteq \tilde{\mathcal{B}}. \quad (32)$$

where the notations are same with those in Section 3.2.

For any subject  $O$  in set  $\mathcal{B}_1$  and also appearing in other  $n - 1$  sub-sets in  $\tilde{\mathcal{B}}$ . Based on the transitivity property in Eq. (6) in Section 3.2, we define a transitive operation by circularly passing through all these  $n$  sets as

$$\Phi_{\mathcal{B}_1} \triangleq \varphi_{\mathcal{B}_1\mathcal{B}_2} \triangleleft \varphi_{\mathcal{B}_2\mathcal{B}_3} \triangleleft \cdots \triangleleft \varphi_{\mathcal{B}_{n-1}\mathcal{B}_n} \triangleleft \varphi_{\mathcal{B}_n\mathcal{B}_1}. \quad (33)$$

Note that, here we do not assume that all the sets share the same persons. Thus,  $\Phi_{\mathcal{B}_1}$  is not an identity mapping like Eq. (6). We take advantage of the universal set  $\mathcal{U}$  in Eq. (32) and get

$$\Phi_{\mathcal{B}_1} = \varphi_{\mathcal{B}_1\mathcal{U}} \triangleleft \varphi_{\mathcal{U}\mathcal{B}_2} \triangleleft \cdots \triangleleft \varphi_{\mathcal{B}_n\mathcal{U}} \triangleleft \varphi_{\mathcal{U}\mathcal{B}_1}, \quad (34)$$

in which we plug in the variable  $O$  and get the result of the transitive association relations as

$$\Phi_{\mathcal{B}_1}(O) = \varphi_{\mathcal{U}\mathcal{B}_1}(\varphi_{\mathcal{B}_n\mathcal{U}}(\cdots \varphi_{\mathcal{U}\mathcal{B}_2}(\varphi_{\mathcal{B}_1\mathcal{U}}(O))))). \quad (35)$$

On the other hand, since  $O$  appears in all  $n$  sets, we can easily get

$$\varphi_{\mathcal{B}_j\mathcal{U}}(\varphi_{\mathcal{U}\mathcal{B}_j}(\varphi_{\mathcal{B}_i\mathcal{U}}(O))) = \varphi_{\mathcal{B}_i\mathcal{U}}(O), \forall \mathcal{B}_i, \mathcal{B}_j \subseteq \tilde{\mathcal{B}}. \quad (36)$$

From the above two equations, we can get

$$\Phi_{\mathcal{B}_1}(O) = \varphi_{\mathcal{U}\mathcal{B}_1}(\varphi_{\mathcal{B}_1\mathcal{U}}(O)) = O. \quad (37)$$

So far, the connection of subject  $O$  forms a closed loop. ■

Next, we discuss how to use a differentiable loss to model Eq. (31). According to the theory of matrix, if  $\mathbf{A}$  is a real symmetric matrix (guaranteed by the constraint of symmetric-consistency), Equation (31) is equivalent to  $\mathbf{A}$  being **positive-semidefinite** [61]. It can be proved that we can use the nuclear norm  $\|\mathbf{A}\|_*$  (i.e., the sum of singular values) to approximate the above constraint of  $\mathbf{A}$ .

**Inference.** Let  $\mathbf{e} = (e_1, e_2, \dots, e_N)$  denote the eigenvalues of  $\mathbf{A}$ , from the knowledge of matrix theory we can know that when  $\mathbf{A}$  is a real symmetric matrix, its singular value is equal to the absolute value of the eigenvalue, then we can get

$$\|\mathbf{A}\|_* = \|\mathbf{e}\|_1, \quad (38)$$

which represent the sum of the absolute values of the eigenvalues.

For positive-semidefinite constraint, we want  $e_i \geq 0, \forall i \in \{1, 2, \dots, N\}$ , we know  $|e_i| \geq e_i$ , then we can minimize  $|e_i| - e_i, \forall i \in \{1, 2, \dots, N\}$  to guarantee that, i.e. minimizing  $\sum_{i=1}^N (|e_i| - e_i)$ . Here we have

$$\sum_{i=1}^N (|e_i| - e_i) = \sum_{i=1}^N |e_i| - \sum_{i=1}^N e_i = \|\mathbf{A}\|_* - \text{tr}(\mathbf{A}), \quad (39)$$

with the constraint of  $\mathcal{L}_{\text{Pse}}^{\text{M}}$ , each of the diagonal elements in  $\mathbf{A}$  is close to 1, i.e.  $\text{tr}(\mathbf{A})$  is close to  $N$ . So we can only minimize  $\|\mathbf{A}\|_*$  to guarantee positive-semidefinite constraint. ■

This way, we use the nuclear norm to approximately guarantee the transitive-consistency

$$\mathcal{L}_{\text{Trs}}^{\text{M}} = \|\mathbf{A}\|_*. \quad (40)$$

### 3.5 The New Association and Tracking Scheme

With the above spatial-temporal self-consistency for appearance learning in Section 3.3 and assignment matrix learning in Section 3.4, our method can be trained with the videos without tracking and association labels. The total loss of the whole framework is calculated as

$$\mathcal{L} = \mathcal{L}_{\text{Sym}}^{\text{A}} + \mathcal{L}_{\text{Trs}}^{\text{A}} + \mathcal{L}_{\text{Pse}}^{\text{M}} + \mathcal{L}_{\text{Sym}}^{\text{M}} + \mathcal{L}_{\text{Trs}}^{\text{M}}. \quad (41)$$

In the inference stage, we propose a new scheme to jointly achieve the association and tracking tasks. After getting the output  $\mathbf{A}$  of STAN, we partition the matrix according to different time and views, on each of which uses the Hungarian algorithm with matching threshold  $M$  to get the binary matrix as the final spatial

permutation matrices. For temporal association, we use the cascade matching and IOU matching for temporal subject association following the MOT algorithm DeepSort [62]. Considering the space occupation and running speed, we use the frames from two consecutive points of time and all views to generate the spatial-temporal affinity matrix as the input of STAN in the training and inference. The proposed MvMHAT scheme is summarized in Algorithm 1. Specifically for the human ID assignment strategy, let's explain it by an example. In view  $v_1$ , we assume a person  $P$  firstly appears at time  $t_1$ , then disappears at  $t_2$ , and re-appears at  $t_3$ . In this case, at  $t_1$ , we use Algorithm 1 to assign a new ID to  $P$  and initialize a multi-view tracklet. At  $t_2$ , we mark the unmatched tracklet to be 'sleep' in view  $v_1$ . Here the tracklet of subject  $P$  in  $v_1$  interrupts but the multi-view tracklet of  $P$  maintains because it still appears in other views. At  $t_3$ , we use the multi-view subject association results to help match  $P$  to the slept tracklet in view  $v_1$ . For the traditional MOT, it is hard to continuously track  $P$  if it disappears for a long time –  $P$  is usually assigned with a new ID when it re-appears.

---

#### Algorithm 1: MvMHAT framework:

---

**Input:**  $\mathcal{V} = \{\mathcal{V}_i | i = 1, \dots, V\}$ : a group of synchronized videos captured from different  $V$  views.

**Output:** Tracked subject bounding boxes with associated ID.

```

1 for  $t = 1 : T$  do
2   for  $t = 1 : T$  do
3     Detect the  $N_t^v$  subjects in frame  $t$  for each view  $v$ :
        $\mathcal{B}_t^v = \{B_{t,j}^v | j = 1, 2, \dots, N_t^v\} (v = 1, 2, \dots, V)$ .
4     Generate features  $\tilde{\mathbf{E}}$  from the matched trajectories in
       previous frames and  $\mathcal{B}_t^v$  at frame  $t$  in each view  $v$ .
5     Generate  $\tilde{\mathbf{X}}$  from  $\tilde{\mathbf{E}}$  according to Section 3.4.1.
6      $\mathbf{A} = \text{STAN}(\tilde{\mathbf{X}})$ 
7      $\mathbf{A} = \frac{1}{2}(\mathbf{A} + \mathbf{A}^T)$ 
8     Generate spatial permutation matrices
        $\mathbf{P}_{t,t}^{v,u}, \mathbf{P}_{t,t-1}^{v,u} (v, u = 1, 2, \dots, V; v \neq u)$  from  $\mathbf{A}$ .
9     for  $v = 1 : V$  do
10      // temporal association
11      tracker[ $v$ ].unmatchdets, tracker[ $v$ ].matches =
12      DeepSort(tracker[ $v$ ].tracks,  $\mathbf{E}_t^v, \mathcal{B}_t^v$ )
13      for  $v = 1 : V$  do
14        for  $p \in \text{tracker}[v].\text{unmatchdets}$  do
15          // spatial association using the
16          // current and previous frames
17          if  $(\exists u, q, \mathcal{T}_q, s.t. \mathbf{P}_{t,t}^{v,u}(p, q) = 1 \wedge (\mathcal{T}_q, q) \in$ 
18          tracker[ $u$ ].matches)  $\vee (\exists u (u \neq$ 
19           $v), \mathcal{T}_q, s.t. \mathbf{P}_{t,t-1}^{v,u}(p, \mathcal{T}_q) = 1)$  then
20            tracker[ $v$ ].matches.add( $(\mathcal{T}_q, p)$ )
21            if  $\mathcal{T}_q \notin \text{tracker}[v].\text{tracks}$  then
22              tracker[ $v$ ].tracks.add( $\mathcal{T}_q$ )
23          else
24            Initialize new tracklet  $\mathcal{T}_p$  with  $\mathcal{B}_{t_p}^v$ .
25            tracker[ $v$ ].tracks.add( $\mathcal{T}_p$ )
26            tracker[ $v$ ].matches.add( $(\mathcal{T}_p, p)$ )
27      tracker[ $v$ ].unmatchdets.remove( $p$ )
28 return Bounding boxes with ID numbers in tracks

```

---

### 3.6 Implementation Details

**Network settings.** We use annotated detection while training and use results of Detectron [63] while inference. We use ResNet-50 [64] as the feature extraction backbone network in all experiments, which has outputs of 1000-d features. In Eq. (9), we set



$\epsilon = 0.1$  and  $\delta = 0.5$ . The parameters  $M$  in Eq. (19),  $m_1$  in Eq. (21), and  $m_2$  in Eq. (22) are set as 0.5, 0.5 and 0.4, respectively. In Eq. (28), we set  $\gamma = 2$  and  $\alpha$  is calculated from the ratio of negative samples to total samples. We use the Pytorch backend for implementing the proposed network and run it on a computer with RTX 3090 GPU. Our network is trained on 8700 groups of frames in MvMHAT training dataset and 8000 groups of frames in MMP-MvMHAT training dataset for 15 epochs with the initial learning rate  $10^{-5}$ .

**STAN pre-training strategy.** We also develop a self-supervised pre-training strategy for STAN by automatically generating the training data. i.e., input matrix  $\tilde{\mathbf{X}}$  and ground-truth assignment matrix  $\mathbf{A}^{\text{gt}}$ . Specifically, we simulate the multi-view multi-subject scene and generate the multi-view over-time subject assignment matrix  $\mathbf{A}^{\text{gt}}$ , on which we add the random noise to obtain the input matrix  $\tilde{\mathbf{X}}$ . We constrain the row sum of each submatrix  $\mathbf{X}_{t,s}^{u,v}$  in  $\tilde{\mathbf{X}}$  as 1 to simulate the results obtained by the row softmax operation. We also define a controllable parameter error rate  $e_r$ , which considers the probability of occurrence, i.e., the same person in different frames show big appearance difference while the different person show the similar difference. In the experiments, we perform the end-to-end training using the framework of Fig. 2 with the pre-train STAN using above strategy and the STAN without pre-training, respectively.

## 4 MvMHAT BENCHMARK

### 4.1 Datasets

#### 4.1.1 A new MvMHAT dataset

**Dataset Collection.** To the best of our knowledge, most previous MOT datasets with multiple views covering an overlapped region are relatively small and only used for algorithm testing. For both training and testing the proposed framework, we build an exclusive large-scale video dataset – MvMHAT benchmark, for multi-view multi-human association and tracking task. For reducing the cost of data collection and annotation while maintaining the usefulness and credibility of the proposed dataset, some videos and corresponding annotations in MvMHAT are from two available datasets, i.e., Campus [41], EPFL [7]. Besides, we have also collected 12 video groups containing 46 sequences, with each group has three to four views. To enrich the way of data collection, different from previous videos captured by fixed cameras, these videos are collected with four wearable cameras, i.e., GoPro, which cover an overlapped area present with multiple people and are from significantly different directions, e.g., near 90-degree view-angle difference. We then manually synchronize them and annotate the bounding box and the ID for each subject on all 30,900 frames.

TABLE 1  
Data source and statistics of MvMHAT dataset.

Source	Campus	EPFL	Self Collected	Total
# Group	6	8	12	26
# Sequence	22	30	46	98
# View	3-4	3-4	3-4	3-4
Avg. Length	1500	900	672	928
Avg. Subject	14	8	10	10
Sum. Length	33,000	27,000	30,900	90,900

**Dataset statistics and splitting.** As shown in Table 1, in total, the dataset in MvMHAT contains 26 multi-view video groups with

98 (single-view) sequences. Each video group contains several temporal-synchronized videos with multiple views, e.g., 3 – 4 views. The average length of each sequence is 928 frames, and average ten subjects appear in each video. The dataset, in total, contains over 90 thousand frames. We further split the dataset into training and testing datasets, each of which contains 13 video groups, and the ratio of containing frames in the training and the testing datasets is about 2:1. To guarantee the diversity of the testing data, the testing videos contain the videos from Campus, EPFL, and Self collected.

#### 4.1.2 MMP-MvMHAT dataset

**Dataset description.** A recent challenge has collected a new dataset namely Multi-camera Multiple People Tracking (MMPTRACK) [65], which aims to tackle multiple people tracking using multiple RGB cameras. It provides long continuous videos that can be used to track people in relatively closed, tight, and complex scenes for long periods of time. All videos are recorded by multiple cameras at different locations in an indoor scene, e.g., retail, lobby, industry, cafe and office (each scene has 4-6 cameras), where each camera has the overlapping field of view (FOV) with at least one of the other cameras. Each scene is divided into four half-day sessions for recording (two sessions for training, one session for validation, and one session for testing). In total, this dataset has 28 people with different genders, ages and guarantees the training, validation and testing sets don't have the same people. Due to environments are crowded and cluttered, the occlusion of people occurs frequently, and in some scenes, such as industry, people wear the same work clothes and have similar appearance difference, which makes this dataset very challenging.

**Dataset reconstitution.** MMPTRACK dataset provides two sub-tracking challenges: 1) top-down view tracking; 2) single-view tracking separately, both of which are different from our simultaneous association and tracking task. This way, based on the original MMPTRACK dataset, we reconstruct a new MMP-MvMHAT dataset and include it for evaluating our task. In order to ensure that the MMP-MvMHAT and MvMHAT datasets have approximate data scale, we choose the first 2,000 frames of the four scenes of the lobby, industry, cafe and office videos from all two half-day sessions in the original training set to build ours (i.e. total 8,000 groups of frames for training). Since the origin testing set does not provide ground truth annotation and we need to use our own metrics for evaluation, we use the original validation set to build our test set. We use the first 1,000 frames of the four scenes mentioned above from one half-day session in the original validation set as our testing set (i.e. total 4,000 frames for testing). In MMP-MvMHAT dataset we use the annotated subject detection boxes for training and testing in the experiments. Note that, we do not use the calibration information of the cameras to fit the more general multi-view camera settings.

### 4.2 Evaluation metrics

**MHT metrics.** We first apply the commonly used MOT metric, i.e., multiple object tracking accuracy (MOTA) proposed in [66] for the single-view tracking performance evaluating as in MOT Challenge [67]. A key task of the MvMHAT task is to associate and track the same subject along the time. We are more concerned about the ID related metrics [33] - ID precision (IDP), ID recall (IDR), and ID F<sub>1</sub> measure (IDF<sub>1</sub>) in evaluation. We also include a new but effective metric – High Order Tracking

Accuracy (HOTA) [68], which explicitly balances the effects of performing accurate detection, association and localization into a single unified metric to evaluate the MOT performance.

**MvMHA metrics.** We further apply the metrics for cross-view association evaluation, i.e., AIDP, AIDR, and AIDF<sub>1</sub>, by expanding the cross-view association metrics in [4], [9]. Specifically, AIDP and AIDR denote the multi-view subject association precision and recall, respectively. Given the subject IDs in all views, we take two views each time and compute the pairwise subject matching performance as in [4], [9], whose average on all views is used as a multi-view association metric. Based on AIDP and AIDR, the association F<sub>1</sub> score is computed as  $AIDF_1 = \frac{2 \times AIDP \times AIDR}{AIDP + AIDR}$ . Following [4], [66], we also apply multi-view multi-human association accuracy MHAA =  $1 - \frac{\sum_t (MS_t + FP_t + 2MM_t)}{\sum_t N_t}$ , where MS<sub>t</sub>, FP<sub>t</sub>, MM<sub>t</sub> are the false negative, false positive, and mismatched pairs at frame *t*. N<sub>t</sub> is the total number of subjects within all views at time *t*. The MHAA follows the definition and calculation pattern of MOTA.

**MvMHAT metrics.** For the overall performance evaluation of MvMHAT problem, we first take a simple average and get the MvMHAT F<sub>1</sub> score, i.e.,  $\mathcal{F} = \text{mean}(\text{IDF}_1, \text{AIDF}_1)$  and MvMHAT accuracy score, i.e.,  $\mathcal{A} = \text{mean}(\text{MOTA}, \text{MHAA})$ . We also define a new metric STMA (Spatial-Temporal Matching Accuracy) for MvMHAT evaluation. Given a time window with the length *t*, we first generate the ground-truth matching and the corresponding predicted spatial-temporal subject matching matrix defined in Eq. (27), which include both the cross-view and over-time subject association result across all views for consecutive *t* frames. We use the human bounding box overlap to establish the subject correspondence between the two matrices, we also use zero padding on the FP (FN) subject matching results in ground truth (predicted) matching matrix to make them the same size. Then we calculate the F<sub>1</sub> score between them. By sliding the time window with the step of  $\frac{t}{2}$  through the whole video, F1 is calculated for each time window and averaged to obtain the final result as STMA score. We set *t* = 5, 10, 30 and get S@5, S@10 and S@30 to evaluate the MvMHAT performance of the tracker for short, medium and medium-long time periods.

## 5 EXPERIMENTAL RESULTS

### 5.1 Comparison Results

#### 5.1.1 Baseline methods

As discussed above, we actually did not find existing methods that can directly handle our MvMHAT problem for comparison. Therefore, we try to include sufficient related approaches with some modifications for comparison.

- We first select four state-of-the-art MOT methods for single-view video, including CenterTrack [19], Tracktor++ [20], TraDeS [21] and TrackFormer [24] for comparison. We know that the single-view MOT methods only handle the tracking in each video but not including the cross-view association. For comparison, we additionally help them by providing the ground-truth unified IDs for the subjects among different views when they appear in each video for the first time. The over-time tracking on each video can propagate the IDs to subsequent frames, which we can use to associate the subjects across views and over time.
- We also include two methods on multi-camera multi-human tracking for comparison, i.e., DeepCC [13] and SVT [5]. Note that, DeepCC is used to handle the human tracking and re-identification

(re-id) using multiple cameras covering different areas. We modify it to handle the proposed MvMHAT following its basic idea of using deep re-id features and clustering algorithm. Specifically, we use an off-the-shelf person re-identification method [69] trained on the Market-1501 dataset [70] as the feature extraction network to extract the appearance feature of each human bounding box. Then as originally we construct  $\tilde{\mathbf{X}}$  using two consecutive points of time and all views subjects. We use the spectral clustering to generate spatial-temporal permutation matrices  $\mathbf{P}$  as the MvMHAT result, where we additionally provide the ground truth number of persons contained in each  $\tilde{\mathbf{X}}$  as clusters number. For SVT, we solve  $\mathbf{P}$  for the symmetric and cycle consistency constraints using the Augmented Lagrangian Method (ALM) algorithm as in [5]. We also modified these two methods based on the inference framework in Algorithm 1 as our method for fair comparison.

- Besides, we also compared with the prior version of this work in [10], i.e. a self-supervised method that does not consider the dummy nodes and the spatial-temporal global information in the assignment matrix generation.

For a fair comparison, we use the same human detection provided by the commonly used detector [63] in MvMHAT dataset and use annotation detections in MMP-MvMHAT dataset, for all the comparison methods and the proposed method. We also reserve the results provided by CenterTrack and TraDeS using the private detector denoted as (P), as shown in Tables 2 and 3. We clarify that all the networks in the comparison methods we use are the public version trained on the original training dataset. For relatively fair, we use the trained models of the comparison methods and do not re-train them on our datasets, since all these methods need supervision with labeled data, which is not used in our self-supervised method.

#### 5.1.2 Results on MvMHAT dataset

Table 2 shows the comparative results of our methods with the baseline methods. For the single-view MOT methods, i.e., Tracktor++, CenterTrack, TraDes and TrackFormer, we first evaluate the over-time tracking performance using the standard MOT metrics. We can see that the state-of-the-art approach TraDes with the private detector provide the best MOTA score among all competitors. Note that, MOTA mainly focuses on the object detection accuracy and precision during tracking [68]. On the contrary, the ID-based metrics, i.e., IDP, IDR and IDF<sub>1</sub> evaluate the ID association and consistency over time. This paper is more concerned about the latter. We can see that the proposed method outperforms all the above methods in IDF<sub>1</sub> score. The composite metric HOTA also demonstrates the effectiveness of our method for over-time tracking. We then show the cross-view association results in the middle of Table 2. From the first six rows, we can see that the cross-view association performances provided by the single-view MOT methods are poor even with the help of providing the ground-truth unified IDs for the subjects among different views for the first time. This is because, without the cross-view re-associating mechanism during tracking, the association will fail once occurring the subject ID switch.

For the first two multi-view tracking approaches, i.e., DeepCC and SVT, which have significantly better ability to associate across view, but are still worse than our method. This is because our method is an end-to-end training framework that not only generates assignment results using spatial-temporal global consistency information, but also use it to train the feature extraction network simultaneously, while DeepCC and SVT are two-stage methods

TABLE 2  
Comparative results of different methods on the proposed MvMHAT benchmark.

Method	Over-Time Tracking					Cross-View Association				Overall				
	IDP	IDR	IDF <sub>1</sub>	MOTA	HOTA	AP	AR	AF <sub>1</sub>	MHAA	$\mathcal{A}$	$\mathcal{F}$	$\mathcal{S}@5$	$\mathcal{S}@10$	$\mathcal{S}@30$
Tracktor++ [20]	54.2	40.1	46.1	66.5	42.8	34.3	14.6	20.5	37.1	51.8	33.3	44.9	44.2	42.5
CenterTrack [19]	44.3	33.5	38.1	63.5	37.8	29.7	9.1	13.9	34.1	48.8	26.0	42.3	41.4	38.9
TraDeS [21]	46.7	43.2	44.9	69.5	42.9	32.4	14.0	19.6	36.0	52.8	32.2	48.5	47.8	45.8
TrackFormer [24]	52.3	47.2	49.6	70.4	47.3	47.8	23.2	31.3	40.2	55.3	40.4	54.2	53.6	51.9
CenterTrack (P)	43.8	33.7	38.1	63.1	37.7	31.9	9.3	14.4	34.3	48.7	26.3	42.8	41.9	39.4
TraDeS (P)	53.9	50.5	52.1	<b>70.8</b>	46.8	38.7	19.7	26.1	38.5	54.7	39.1	51.5	50.9	49.2
DeepCC [13]	44.7	44.2	44.4	63.9	41.1	57.9	34.8	43.4	43.8	53.9	43.9	56.6	55.6	52.8
SVT [5]	47.9	47.2	47.6	65.4	43.1	61.7	45.7	52.5	50.4	57.9	50.0	61.4	60.5	58.4
Prior [10]	53.1	52.0	52.5	64.7	47.9	53.0	46.4	49.5	51.7	58.2	51.0	60.4	59.5	58.1
Ours	<b>58.5</b>	<b>57.4</b>	<b>57.9</b>	66.3	<b>51.8</b>	<b>63.8</b>	<b>56.0</b>	<b>59.6</b>	<b>59.7</b>	<b>63.0</b>	<b>58.8</b>	<b>67.1</b>	<b>66.3</b>	<b>65.0</b>

TABLE 3  
Comparative results of different methods on MMP-MvMHAT benchmark.

Method	Over-Time Tracking					Cross-View Association				Overall				
	IDP	IDR	IDF <sub>1</sub>	MOTA	HOTA	AP	AR	AF <sub>1</sub>	MHAA	$\mathcal{A}$	$\mathcal{F}$	$\mathcal{S}@5$	$\mathcal{S}@10$	$\mathcal{S}@30$
Tracktor++ [20]	67.0	56.0	61.0	67.2	46.2	62.0	23.2	33.8	19.1	43.1	47.4	45.2	44.7	43.8
CenterTrack [19]	35.9	24.1	28.8	48.2	27.1	29.3	3.9	6.8	3.1	25.7	17.8	26.0	25.0	23.0
TraDeS [21]	59.7	50.1	54.5	66.1	42.7	54.5	17.3	26.2	13.3	39.7	40.4	41.5	41.0	40.2
TrackFormer [24]	41.8	28.6	34.0	46.7	30.2	39.9	5.3	9.4	3.2	25.0	21.7	27.2	26.6	25.1
CenterTrack (P)	31.9	24.1	27.4	39.6	26.1	32.6	3.7	6.7	3.1	21.3	17.1	25.7	24.8	22.8
TraDeS (P)	57.3	49.8	53.3	63.0	42.0	53.1	17.1	25.9	13.2	38.1	39.6	41.0	40.5	39.7
DeepCC [13]	51.6	52.5	52.1	92.5	59.3	42.7	23.4	30.2	19.7	56.1	41.2	47.3	46.4	43.1
SVT [5]	63.1	63.4	63.3	<b>96.7</b>	68.8	53.8	33.4	41.2	29.8	63.1	52.3	55.6	55.0	53.3
Prior [10]	58.6	58.8	58.7	93.7	65.0	35.4	21.2	26.5	20.3	57.0	42.6	44.7	44.0	41.8
Ours	<b>67.1</b>	<b>67.6</b>	<b>67.3</b>	95.0	<b>70.2</b>	<b>62.1</b>	<b>42.5</b>	<b>50.4</b>	<b>40.6</b>	<b>67.8</b>	<b>58.9</b>	<b>61.8</b>	<b>61.2</b>	<b>59.3</b>

and consider spatial-temporal association only in the assignment phase. Compared to the prior version of our method, the results are further improved. This is because we consider the more general and frequent dummy nodes cases caused by the occlusion or out of view, and we also take advantage of the spatial-temporal global consistency information in the assignment phase. For the overall performance metrics, i.e.,  $\mathcal{A}$ ,  $\mathcal{F}$  and  $\mathcal{S}$ , on all of which our method get the best performance. This significantly verify the effectiveness of the proposed method for MvMHAT problem.

### 5.1.3 Results on MMP-MvMHAT dataset

Table 3 shows the comparative results of our methods with the baseline methods. Since MMP-MvMHAT dataset is a simulated indoor scene dataset, the subjects in it have simpler motion patterns. In some scenes, such as the office scene, many subjects even do not walk around, but just work in their seats. So compared to Table 2, we can see that most of the methods have higher IDF<sub>1</sub> score in over-time tracking except CenterTrack and TrackFormer. For the single-view MOT methods Tracktor++ and TraDes, with the over-time tracking becomes more accurate, the corresponding cross-view association AIDF<sub>1</sub> scores are also improved. However, for CenterTrack, since the method only uses the subjects of two adjacent frames for association and does not use the appearance features of the subjects, in crowded and complex scenes, i.e., when the subjects are close with frequent mutual occlusions, Centertrack often generates ID switch in the over-time tracking, resulting in poor MOT results. We also note that TrackFormer performs not very well on MMP-MvMHAT, especially for MOTA. TrackFormer is a algorithm that implements both human detection

and association. This way, even if we provide the unified human detection results, it only filters its own detection results based on them. Thus the inaccurate detection result of TrackFormer on MMP-MvMHAT dataset makes the tracking results unsatisfactory. Their poor MOT results also lead to poor cross-view association results accordingly.

For the multi-view tracking approaches, we are able to find that the performance of cross-view association of these methods decreases compared to Table 2, because the humans in this dataset have similar appearance, and the human bounding boxes always contain cluttered backgrounds or other objects. This will interfere with the effectiveness of extracted subject features, making the approach using appearance similarity for association is incompetent on this dataset. We can also find that our ‘prior’ method does not work well on this dataset, because it does not use the spatial-temporal global consistency information when cross-view association, but only uses the similarity of subject appearance between pairwise views to obtain association results, while the appearance feature is no longer reliable for this dataset as discussed above. This also illustrates the effectiveness of our improvements made in this work, even in complex and crowded scenes our method still works well. For the overall performance metrics, i.e.,  $\mathcal{A}$ ,  $\mathcal{F}$  and  $\mathcal{S}$ , on all of which our method performs best among all methods.

## 5.2 Ablation Study

### 5.2.1 Effectiveness of self-supervised loss

We first investigate the effectiveness of self-supervised loss by considering the following ablation studies.

TABLE 4  
Ablation study of different variations of our method on MvMHAT benchmark.

Method	Over-Time Tracking					Cross-View Association				Overall				
	IDP	IDR	IDF <sub>1</sub>	MOTA	HOTA	AP	AR	AF <sub>1</sub>	MHAA	$\mathcal{A}$	$\mathcal{F}$	S@5	S@10	S@30
w/o Training	32.9	33.4	33.2	56.7	33.2	21.6	14.6	17.4	27.6	42.1	25.3	37.3	35.7	30.8
w/o $\mathcal{L}_{\text{Sym}}^{\text{A}}$	56.4	55.5	55.9	65.3	50.5	62.2	55.4	58.6	58.1	61.7	57.3	66.1	65.2	63.7
w/o $\mathcal{L}_{\text{Trs}}^{\text{A}}$	54.8	53.8	54.3	65.2	50.0	61.6	55.7	58.5	58.4	61.8	56.4	66.2	65.3	63.8
w/o dummy nodes	56.2	55.2	55.7	66.4	49.3	57.8	50.8	54.1	56.2	61.3	54.9	64.1	63.3	61.9
w/o $\mathcal{L}_{\text{Sym}}^{\text{M}}$	57.5	56.4	57.0	66.4	51.5	60.5	52.0	55.9	57.2	61.8	56.5	65.0	64.2	63.0
w/o $\mathcal{L}_{\text{Trs}}^{\text{M}}$	58.1	57.0	57.5	66.4	52.4	61.1	54.3	57.5	57.9	62.1	57.5	66.0	65.2	63.9
w/o Association	64.9	<b>63.2</b>	<b>64.0</b>	<b>67.9</b>	<b>55.3</b>	42.9	3.5	6.5	30.3	49.1	35.2	44.7	43.9	42.7
w/o Tracking	<b>65.8</b>	45.8	54.0	47.8	46.1	<b>68.2</b>	52.0	59.0	56.4	52.1	56.5	59.2	58.2	56.7
Ours	58.5	57.4	57.9	66.3	51.8	63.8	<b>56.0</b>	<b>59.6</b>	<b>59.7</b>	<b>63.0</b>	<b>58.8</b>	<b>67.1</b>	<b>66.3</b>	<b>65.0</b>

TABLE 5  
Ablation study of STAN with different settings on MvMHAT benchmark.

Method	Over-Time Tracking					Cross-View Association				Overall				
	IDP	IDR	IDF <sub>1</sub>	MOTA	HOTA	AP	AR	AF <sub>1</sub>	MHAA	$\mathcal{A}$	$\mathcal{F}$	S@5	S@10	S@30
w/o STAN	57.5	56.4	56.9	66.0	50.9	<b>64.0</b>	53.3	58.2	57.3	61.6	57.5	66.0	65.2	63.9
w one time point	58.3	57.1	57.7	66.3	51.3	63.9	52.2	57.5	57.0	61.6	57.6	65.8	65.0	63.9
unpretrain STAN	57.3	56.2	56.8	66.1	51.5	59.3	53.2	56.1	57.3	61.7	56.4	64.7	63.9	62.5
$e_r = 0.05$	56.4	55.3	55.8	66.3	51.0	61.5	55.8	58.5	58.6	62.5	57.2	66.2	65.4	64.0
$e_r = 0.15$	58.1	57.0	57.5	65.9	<b>52.3</b>	61.4	55.9	58.5	58.7	62.3	58.0	66.3	65.5	64.2
$e_r = 0.30$	56.9	55.8	56.4	66.2	51.1	60.5	54.8	57.5	58.1	62.1	56.9	66.1	65.3	63.9
Ours ( $e_r = 0.10$ )	<b>58.5</b>	<b>57.4</b>	<b>57.9</b>	<b>66.3</b>	51.8	63.8	<b>56.0</b>	<b>59.6</b>	<b>59.7</b>	<b>63.0</b>	<b>58.8</b>	<b>67.1</b>	<b>66.3</b>	<b>65.0</b>

- w/o Training: We directly use the Resnet-50 pre-trained on ImageNet [71] and STAN pre-trained on synthetic dataset (with  $e_r = 10\%$ ) without using the self-supervised training proposed in our method.
- w/o  $\mathcal{L}_{\text{Sym}}^{\text{A}}$ : Remove the symmetric-consistency loss for appearance feature learning  $\mathcal{L}_{\text{Sym}}^{\text{A}}$  in Eq. (24).
- w/o  $\mathcal{L}_{\text{Trs}}^{\text{A}}$ : Remove the transitive-consistency loss for appearance feature learning  $\mathcal{L}_{\text{Trs}}^{\text{A}}$  in Eq. (25).
- w/o dummy nodes: Use a diagonal identity matrix to supervise  $\mathbf{I}$  with a relaxation [10] instead of Eq. (23).
- w/o  $\mathcal{L}_{\text{Sym}}^{\text{M}}$ : Remove the symmetric-consistency loss for assignment matrix learning  $\mathcal{L}_{\text{Sym}}^{\text{M}}$  in Eq. (30).
- w/o  $\mathcal{L}_{\text{Trs}}^{\text{M}}$ : Remove the transitive-consistency loss for assignment matrix learning  $\mathcal{L}_{\text{Trs}}^{\text{M}}$  in Eq. (40).

As shown in Table 4, we can see that ‘w/o Training’ has a poor performance, which shows the challenge of the MvMHAT task and the importance of proposed self-supervised training. Our loss functions enable the network to unsupervised find the potential characteristics of data. ‘w/o  $\mathcal{L}_{\text{Sym}}^{\text{A}}$ ’ and ‘w/o  $\mathcal{L}_{\text{Trs}}^{\text{A}}$ ’ make over-time tracking results drop significantly, this means we can’t have one without the other, in which  $\mathcal{L}_{\text{Sym}}^{\text{A}}$  only considers the relationship between pairwise frames, while  $\mathcal{L}_{\text{Trs}}^{\text{A}}$  focusing on considering transitive-consistency information. For cross-view association, we still have  $\mathcal{L}_{\text{Sym}}^{\text{M}}$  and  $\mathcal{L}_{\text{Trs}}^{\text{M}}$  losses that also guarantee symmetric-consistency and transitive-consistency, so its results drop little. ‘w/o dummy nodes’ ignores the frequently occurring occlusion or out of view cases, thus leading to the deviation in appearance feature learning with the constrained losses, and the inaccurate feature representation also leads to the degradation of assignment results since matrix  $\mathbf{X}$  also provides the pseudo label for training STAN. ‘w/o  $\mathcal{L}_{\text{Sym}}^{\text{M}}$ ’ and ‘w/o  $\mathcal{L}_{\text{Trs}}^{\text{M}}$ ’ lead to a significant decrease in cross-view association results, which means that only combining

both of them can make better performance. While for over-time tracking, i.e., relying mainly on subject appearance features, they still have  $\mathcal{L}_{\text{Sym}}^{\text{A}}$  and  $\mathcal{L}_{\text{Trs}}^{\text{A}}$  to guarantee symmetric-consistency and transitive-consistency, so the result drop is not very significant.

### 5.2.2 Effectiveness of association and tracking schema

We then investigate the effectiveness of some components in the inference stage by considering the following setting.

- w/o Association: Remove association module during tracking, and generate the association results when the subject first appears.
- w/o Tracking: Remove the collaboratively tracking module, and implement the tracking on one view to obtain the subject ID, in other views by cross-view association.

We can see from Table 4 that ‘w/o Association’ provides very promising tracking results. It can be explained that, without considering the cross-view association, the method under ‘w/o Association’ can avoid more ID switches during tracking. This can be regarded as an upper bound of our method only for tracking, which, however, naturally generates a poor association performance. From comparing the results of ‘w/o Tracking’ and ‘Ours’, we are surprised to find that with the aggregation of tracking, our method not only improves the performance of over-time tracking but also the cross-view association. This inspires us the temporal tracking can be used as a favor for association. Overall, the integration of collaborative tracking & association mechanism generates the best results.

### 5.2.3 Ablation studies on STAN

We also in detail investigate the influence of the proposed STAN and its different variations by considering the following settings.

- w/o STAN: In the inference stage, instead of using the output of STAN to generate spatial permutation matrices  $\mathbf{P}$ ,  $\mathbf{X}$  is used directly to generate  $\mathbf{P}$ .

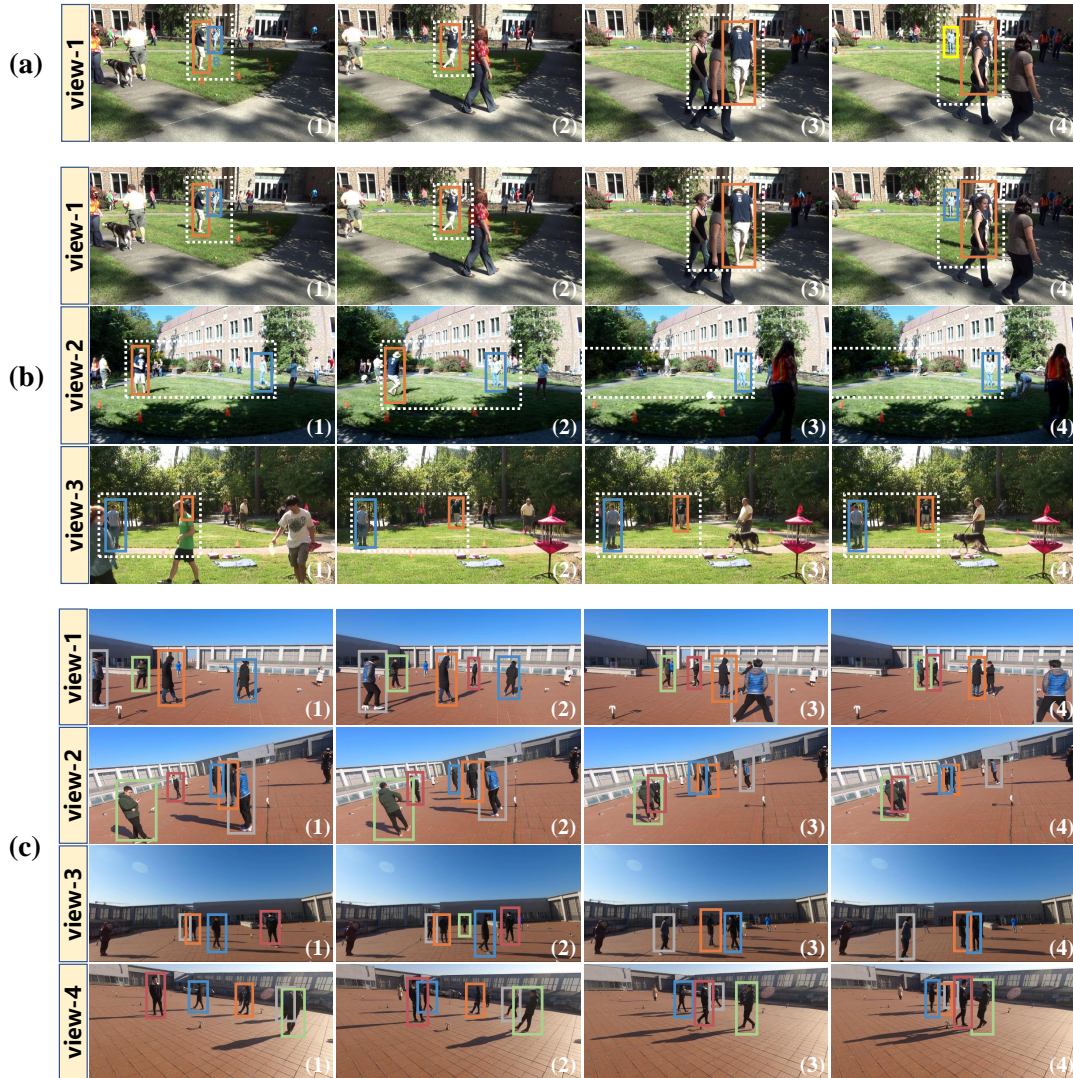


Fig. 5. An illustration of the qualitative results. Figure (a) shows the tracking results of the MOT method Tractor++ for one view, while figure (b) shows the association and tracking results of our method for multiple views. Figure (c) shows the results of our method on a group of multi-view videos in MvMHAT dataset. All the results we show are four sampled frames, which at the same column in each sub-figure are from the same time.

- *w one time point*: In the inference stage, we use the subject bounding boxes in all views at only one point of time (ignoring the over-time information) to generate spatial permutation matrices  $\mathbf{P}$ .
- *unpretrain STAN*: Do not pre-train STAN, initialize parameters with orthogonal matrix.
- $e_r = 0.05, 0.15, 0.30, 0.10$ : Generate pre-training datasets using different error rates  $e_r = 5\%, 15\%, 30\%, 10\%$  and STAN is pre-trained using these datasets respectively.

First, '*w/o STAN*' instead of using STAN network, it only uses appearance feature learning module to extract the subject features and calculate  $\mathbf{X}$  between two frames, then generates the assignment matrix without considering the spatial-temporal global information. We can first see from Table 5 that the drop of the result verifies the effectiveness of the assignment matrix learning module. Compared with prior version of our method in Table 2, we can also find that as an end-to-end framework  $\mathcal{L}_{\text{Sym}}^{\text{M}}$  and  $\mathcal{L}_{\text{Trs}}^{\text{M}}$  losses can also improve the performance of the appearance feature learning module. We can see that '*w one time point*' provides a decreased performance. This is because it considers only spatial consistency without considering temporal consistency

when generating the assignment matrix  $\mathbf{P}$ . Also, it does not use the help of the previous frame when spatial association causing a degradation in the results of cross-view association.

As shown in Table 5, we can see from '*unpretrain STAN*' that even if STAN is trained from scratch, it can still achieve satisfactory results. This is because  $\mathcal{L}_{\text{Sym}}^{\text{A}}$  and  $\mathcal{L}_{\text{Trs}}^{\text{A}}$  losses can ensure the correctness of the appearance feature learning module, and therefore guaranteeing the correctness of the pseudo label generated by  $\tilde{\mathbf{X}}$ , providing STAN network with the correct optimizing direction. As an end-to-end network, assignment matrix learning module can also improve the performance of the appearance feature learning module, forming a virtuous circle. Therefore, the self-supervision method proposed in this work has strong practical application, that is, STAN is not depended on the pre-training. For the pre-trained STAN, we can find that most of the results are better than the unpre-trained STAN, and the results have the best over-time tracking and cross-view association ability when the error rate of the generated dataset  $e_r = 10\%$ . We therefore use this pre-trained STAN model as the initial state of our method on the MvMHAT dataset and MMP-MvMHAT dataset. Note that, as

discussed above, the data for the pre-training of STAN are self-generated without any annotation cost, which does not break the self-supervised manner of this work.

### 5.3 Qualitative Evaluation

Figure 5(a) shows a long-term tracking result of Tracktor++. We can see that two players are practicing baseball in the white dotted area in (1). However, because of the frequent moving of the player A in (2), and comings and goings of pedestrians in (3), the player B is occluded frequently. Thus, the single view MOT methods have to always try to match B with all the tracklets, which leads to lots of incorrect ID switches, e.g., in (4). As shown in Fig. 5(b), our method leverages the complementary characteristic of multiple views, and we ensure that any people can be observed in at least one view at all times. The integration of multi-view tracklets makes good use of both temporal and spatial information. The proposed MvMHAT scheme, to some extent, can help track the re-appearing detections that cannot be matched by the tracking module, while the continual tracking can help associate the subjects that cannot be matched by the association module. This way, a spatial-temporal connection is established for all observed people, which *has the potential to better handle the long-term tracking*. In Fig. 5(c), people are walking and interacting with each other with various activities. Based on the results by MvMHAT, we can capture the details of every people from all-around perspectives. This demonstrates the *potential of the proposed MvMHAT for board applications*, e.g., sports games, indoor/outdoor surveillance, outdoor law enforcement, which aim to capture both global and local details of involved people.

## 6 DISCUSSION

### 6.1 Analysis of Self-supervised Framework

In the training phase, we use  $n$  frames from different time and views as an input batch. For the feature extraction network, as discussed in Section 3.3.2,  $\mathbf{I}_S$  and  $\mathbf{I}_T$  matrices are calculated for any pairwise and triplewise frames among  $n$  frames according to Eqs. (12) and (14). That is, for a batch of  $n$  frames, we generate  $P(n, 2) + P(n, 3)$  matrices for self-supervised learning, where  $P(n, m)$  represents the number of permutations in which  $m$  elements are taken from  $n$  different elements. Considering the space occupation, we use the frames from two consecutive points of time and all views as an batch in our method. Even so, for four views, about 400  $\mathbf{I}$  matrices are generated in each batch, which are constrained by the proposed self-supervised losses  $\mathcal{L}_{\text{Sym}}^A$  and  $\mathcal{L}_{\text{Trs}}^A$  in Eqs. (24) and (25). The feature extraction network is also constrained by  $\mathcal{L}_{\text{Pse}}^M$ ,  $\mathcal{L}_{\text{Sym}}^M$  and  $\mathcal{L}_{\text{Trs}}^M$  of STAN in Eqs. (28), (30), (40) as an end-to-end framework. Therefore, the proposed fully self-supervised learning framework can generate enough self-constraints effectively and be able to produce promising results.

### 6.2 Limitation Analysis

In this paper, we consider the case of inconsistent involved subjects in different views/time. However, when the subjects overlap in different views is too small, i.e., only a very small fraction of the subjects are the same people in each view, the proposed method does not work well. We can see this through the  $\mathcal{L}_{\text{Trs}}^M$  loss in Eqs. (40), i.e., the nuclear norm loss. The nuclear norm is usually used as a convex approximation of the matrix

rank, so we also require the output  $\mathbf{A}$  of STAN to be a low-rank matrix by minimizing the nuclear norm. However, when the overlap across view is very small, i.e.,  $|\mathcal{U}|$  is very close to  $|\mathcal{B}|$ , the ground truth of the spatial-temporal assignment matrix  $\mathbf{A}$  is no longer low-rank. Meanwhile, when the FOV overlap of cameras is very small, the same subject may not appear in multiple cameras at the same time, and cross-view association becomes less important accordingly. This problem is more like the existing MTMCT (multi-target multi-camera tracking) task where the cameras are without FOV overlap. Therefore, we clarify that the proposed MvMHAT problem and the existing MTMCT task *are complementary to each other*, the study on both of which can promote the development of the multi-camera MOT task.

The performance of our method is also related to the number of subjects in the scene and gets worse when there are too many or too few people in each view video. When there are too many subjects, dense crowds can lead to inaccurate subject detection and appearance feature representation results. When there are too few subjects, for the extreme case, when there is only one subject in frame  $j$ , the  $\mathbf{X}_{ij}$  matrix obtained from the row softmax has only one column and each matching score in it is 1, which cannot correctly reflect the matching relation of the subjects between frame  $i$  and frame  $j$ .

## 7 CONCLUSION AND FUTURE WORK

In this paper, we have studied a relatively new problem – MvMHAT, which is different from the existing MOT problem and has promising development potential. For fully excavating the peculiarity of MvMHAT, based on the rationale of spatial-temporal self-consistency, we model this problem as a self-supervised learning task and propose an end-to-end framework to handle it. To promote the study on this new topic, we have also built a couple of MvMHAT benchmarks for network training and performance evaluation. Experimental results verify the rationality of our problem formulation, the usefulness of the proposed benchmark, and the effectiveness of our method.

For future work, we hope to develop more human features to better handle this problem. We mainly explore the appearance consistency of the subjects over time and across views in this work. The input matrix of STAN, i.e., the affinity matrix  $\tilde{\mathbf{X}}$ , is also constructed based on appearance similarity. However, through the comparison between Tables 2 and 3, we can see that the cross-view association result of our method on MMP-MvMHAT dataset is lower than that of MvMHAT dataset. In other words, when the subjects' appearances are similar and the backgrounds are cluttered, our method can not play a good role when only using subject appearance. In fact, the self-consistency constraint proposed in this paper is the consistency of matching relation, not just the consistent appearance similarity. Therefore, in the future, more human features can be explored, such as the consistency of subject pose across views [6] and the consistency of subject motion pattern over time [72]. We can use the proposed self-supervised loss for their consistency learning, so as to better conduct the multi-view multi-human association and tracking. This paper takes the first step to achieve the MvMHAT task using a fully self-supervised method to obtain a promising result. In the future, we hope to develop more research and further attract more interests in the community on this topic.

## REFERENCES

- [1] J. Berclaz, F. Fleuret, E. Turetken, and P. Fua, "Multiple object tracking using k-shortest paths optimization," *IEEE Transactions on Pattern Analysis and Machine Intelligence*, vol. 33, no. 9, pp. 1806–1819, 2011.
- [2] S. Sun, N. Akhtar, H. Song, A. Mian, and M. Shah, "Deep affinity network for multiple object tracking," *IEEE Transactions on Pattern Analysis and Machine Intelligence*, vol. 43, no. 1, pp. 104–119, 2019.
- [3] P. Chu and H. Ling, "FAMNet: Joint learning of feature, affinity and multi-dimensional assignment for online multiple object tracking," in *IEEE International Conference on Computer Vision*, 2019.
- [4] R. Han, W. Feng, Y. Zhang, J. Zhao, and S. Wang, "Multiple human association and tracking from egocentric and complementary top views," *IEEE Transactions on Pattern Analysis and Machine Intelligence*, vol. 44, no. 9, pp. 5225–5242, 2022.
- [5] J. Dong, Q. Fang, W. Jiang, Y. Yang, Q. Huang, H. Bao, and X. Zhou, "Fast and robust multi-person 3d pose estimation and tracking from multiple views," *IEEE Transactions on Pattern Analysis and Machine Intelligence*, vol. 44, no. 10, pp. 6981–6992, 2022.
- [6] M. Vo, E. Yumer, K. Sunkavalli, S. Hadap, Y. Sheikh, and S. G. Narasimhan, "Self-supervised multi-view person association and its applications," *IEEE Transactions on Pattern Analysis and Machine Intelligence*, vol. 43, no. 8, pp. 2794–2808, 2020.
- [7] F. Fleuret, J. Berclaz, R. Lengagne, and P. Fua, "Multicamera people tracking with a probabilistic occupancy map," *IEEE Transactions on Pattern Analysis and Machine Intelligence*, vol. 30, no. 2, pp. 267–282, 2007.
- [8] Y. Xu, X. Liu, L. Qin, and S.-C. Zhu, "Cross-view people tracking by scene-centered spatio-temporal parsing," in *AAAI Conference on Artificial Intelligence*, 2017.
- [9] R. Han, W. Feng, J. Zhao, Z. Niu, Y. Zhang, L. Wan, and S. Wang, "Complementary-view multiple human tracking," in *AAAI Conference on Artificial Intelligence*, 2020.
- [10] Y. Gan, R. Han, L. Yin, W. Feng, and S. Wang, "Self-supervised multi-view multi-human association and tracking," in *ACM Multimedia*, 2021.
- [11] A. Dehghan, S. M. Assari, and M. Shah, "GMMCP Tracker: Globally optimal generalized maximum multi clique problem for multiple object tracking," in *IEEE International Conference on Computer Vision and Pattern Recognition*, 2015.
- [12] Y. Xiang, A. Alahi, and S. Savarese, "Learning to track: Online multi-object tracking by decision making," in *IEEE International Conference on Computer Vision*, 2015.
- [13] E. Ristani and C. Tomasi, "Features for multi-target multi-camera tracking and re-identification," in *IEEE International Conference on Computer Vision and Pattern Recognition*, 2018.
- [14] B. Yang and R. Nevatia, "Multi-target tracking by online learning of non-linear motion patterns and robust appearance models," in *IEEE Conference on Computer Vision and Pattern Recognition*, 2012.
- [15] B. Yang and R. Nevatia, "An online learned CRF model for multi-target tracking," in *IEEE Conference on Computer Vision and Pattern Recognition*, 2012.
- [16] A. R. Zamir, A. Dehghan, and M. Shah, "GMCP-Tracker: Global multi-object tracking using generalized minimum clique graphs," in *European Conference on Computer Vision*, 2012.
- [17] J. Xu, Y. Cao, Z. Zhang, and H. Hu, "Spatial-temporal relation networks for multi-object tracking," in *IEEE International Conference on Computer Vision*, 2019.
- [18] Y. Xu, A. Osep, Y. Ban, R. Horaud, L. Leal-Taixé, and X. Alameda-Pineda, "How to train your deep multi-object tracker," in *IEEE Conference on Computer Vision and Pattern Recognition*, 2020.
- [19] X. Zhou, V. Koltun, and P. Krähenbühl, "Tracking objects as points," in *European Conference on Computer Vision*, 2020.
- [20] P. Bergmann, T. Meinhardt, and L. Leal-Taixé, "Tracking without bells and whistles," in *IEEE International Conference on Computer Vision*, 2019.
- [21] J. Wu, J. Cao, L. Song, Y. Wang, M. Yang, and J. Yuan, "Track to detect and segment: An online multi-object tracker," in *IEEE Conference on Computer Vision and Pattern Recognition*, 2021.
- [22] Y. Zhang, P. Sun, Y. Jiang, D. Yu, F. Weng, Z. Yuan, P. Luo, W. Liu, and X. Wang, "ByteTrack: Multi-object tracking by associating every detection box," in *European Conference on Computer Vision*, 2022.
- [23] G. Brasó and L. Leal-Taixé, "Learning a neural solver for multiple object tracking," in *IEEE Conference on Computer Vision and Pattern Recognition*, 2020.
- [24] T. Meinhardt, A. Kirillov, L. Leal-Taixé, and C. Feichtenhofer, "TrackFormer: Multi-object tracking with transformers," in *IEEE Conference on Computer Vision and Pattern Recognition*, 2022.
- [25] F. Ma, M. Z. Shou, L. Zhu, H. Fan, Y. Xu, Y. Yang, and Z. Yan, "Unified transformer tracker for object tracking," in *IEEE Conference on Computer Vision and Pattern Recognition*, 2022.
- [26] X. Zhou, T. Yin, V. Koltun, and P. Krähenbühl, "Global tracking transformers," in *IEEE Conference on Computer Vision and Pattern Recognition*, 2022.
- [27] A. W. Smeulders, D. M. Chu, R. Cucchiara, S. Calderara, A. Dehghan, and M. Shah, "Visual tracking: An experimental survey," *IEEE Transactions on Pattern Analysis and Machine Intelligence*, vol. 36, no. 7, pp. 1442–1468, 2013.
- [28] G. Ciaparrone, F. L. Sánchez, S. Tabik, L. Troiano, R. Tagliaferrri, and F. Herrera, "Deep learning in video multi-object tracking: A survey," *Neurocomputing*, vol. 381, pp. 61–88, 2020.
- [29] A. Gilbert and R. Bowden, "Tracking objects across cameras by incrementally learning inter-camera colour calibration and patterns of activity," in *European Conference on Computer Vision*, 2006.
- [30] B. J. Prosser, S. Gong, and T. Xiang, "Multi-camera matching using bi-directional cumulative brightness transfer functions," in *British Machine Vision Conference*, 2008.
- [31] Y. Cai and G. Medioni, "Exploring context information for inter-camera multiple target tracking," in *IEEE Winter Conference on Applications of Computer Vision*, 2014.
- [32] X. Chen, K. Huang, and T. Tan, "Object tracking across non-overlapping views by learning inter-camera transfer models," *Pattern Recognition*, vol. 47, no. 3, pp. 1126–1137, 2014.
- [33] E. Ristani, F. Solera, R. Zou, R. Cucchiara, and C. Tomasi, "Performance measures and a data set for multi-target, multi-camera tracking," in *European Conference on Computer Vision*, 2016.
- [34] A. Maksai, X. Wang, F. Fleuret, and P. Fua, "Non-markovian globally consistent multi-object tracking," in *IEEE International Conference on Computer Vision*, 2017.
- [35] Y. T. Tesfaye, E. Zemene, A. Prati, M. Pelillo, and M. Shah, "Multi-target tracking in multiple non-overlapping cameras using fast-constrained dominant sets," *International Journal of Computer Vision*, vol. 127, no. 9, pp. 1303–1320, 2019.
- [36] M. Ayazoglu, B. Li, C. Dicle, M. Sznaiar, and O. I. Camps, "Dynamic subspace-based coordinated multicamera tracking," in *IEEE International Conference on Computer Vision*, 2011.
- [37] S. M. Khan and M. Shah, "A multiview approach to tracking people in crowded scenes using a planar homography constraint," in *European Conference on Computer Vision*, 2006.
- [38] L.-T. Laura, P.-M. Gerard, and R. Bodo, "Branch-and-price global optimization for multi-view multi-target tracking," in *IEEE Conference on Computer Vision and Pattern Recognition*, 2012.
- [39] M. Hofmann, D. Wolf, and G. Rigoll, "Hypergraphs for joint multi-view reconstruction and multi-object tracking," in *IEEE Conference on Computer Vision and Pattern Recognition*, 2013.
- [40] R. Eshel and Y. Moses, "Tracking in a dense crowd using multiple cameras," *International Journal of Computer Vision*, vol. 88, no. 1, pp. 129–143, 2010.
- [41] Y. Xu, X. Liu, Y. Liu, and S. Zhu, "Multi-view people tracking via hierarchical trajectory composition," in *IEEE Conference on Computer Vision and Pattern Recognition*, 2016.
- [42] X. Liu, Y. Xu, L. Zhu, and Y. Mu, "A stochastic attribute grammar for robust cross-view human tracking," *IEEE Transactions on Circuits and Systems for Video Technology*, vol. 28, no. 10, pp. 2884–2895, 2017.
- [43] J. Dong, W. Jiang, Q. Huang, H. Bao, and X. Zhou, "Fast and robust multi-person 3d pose estimation from multiple views," in *IEEE Conference on Computer Vision and Pattern Recognition*, 2019.
- [44] R. Han, Y. Zhang, W. Feng, C. Gong, X. Zhang, J. Zhao, L. Wan, and S. Wang, "Multiple human association between top and horizontal views by matching subjects' spatial distributions," in *arXiv*, 2019.
- [45] K. Zheng, X. Fan, Y. Lin, H. Guo, H. Yu, D. Guo, and S. Wang, "Learning view-invariant features for person identification in temporally synchronized videos taken by wearable cameras," in *IEEE International Conference on Computer Vision*, 2017.
- [46] J. Zhao, R. Han, Y. Gan, L. Wan, W. Feng, and S. Wang, "Human identification and interaction detection in cross-view multi-person videos with wearable cameras," in *ACM Multimedia*, 2020.
- [47] R. Han, J. Zhao, W. Feng, Y. Gan, L. Wan, and S. Wang, "Complementary-view co-interest person detection," in *ACM Multimedia*, 2020.
- [48] R. Zhang, P. Isola, and A. A. Efros, "Colorful image colorization," in *European Conference on Computer Vision*, 2016.
- [49] C. Doersch, A. Gupta, and A. A. Efros, "Unsupervised visual representation learning by context prediction," in *IEEE International Conference on Computer Vision*, 2015.

- [50] X. Wang, A. Jabri, and A. A. Efros, "Learning correspondence from the cycle-consistency of time," in *IEEE Conference on Computer Vision and Pattern Recognition*, 2019.
- [51] Z. Lai and W. Xie, "Self-supervised learning for video correspondence flow," in *British Machine Vision Conference*, 2019.
- [52] M. Li, X. Zhu, and S. Gong, "Unsupervised tracklet person re-identification," *IEEE Transactions on Pattern Analysis and Machine Intelligence*, vol. 42, no. 7, pp. 1770–1782, 2019.
- [53] M. Li, X. Zhu, and S. Gong, "Unsupervised person re-identification by deep learning tracklet association," in *European Conference on Computer Vision*, 2018.
- [54] J. Wu, Y. Yang, H. Liu, S. Liao, Z. Lei, and S. Z. Li, "Unsupervised graph association for person re-identification," in *IEEE International Conference on Computer Vision*, 2019.
- [55] Y. Hou, L. Zheng, Z. Wang, and S. Wang, "Locality aware appearance metric for multi-target multi-camera tracking," in *arXiv*, 2019.
- [56] S. Karthik, A. Prabhu, and V. Gandhi, "Simple unsupervised multi-object tracking," in *arXiv*, 2020.
- [57] K. Ho, J. Keuper, and M. Keuper, "Unsupervised multiple person tracking using autoencoder-based lifted multicuts," in *arXiv*, 2020.
- [58] G. Hinton, O. Vinyals, and J. Dean, "Distilling the knowledge in a neural network," in *arXiv*, 2015.
- [59] Z. Wang, J. Zhang, L. Zheng, Y. Liu, Y. Sun, Y. Li, and S. Wang, "CycAs: Self-supervised cycle association for learning re-identifiable descriptions," in *European Conference on Computer Vision*, 2020.
- [60] T.-Y. Lin, P. Goyal, R. Girshick, K. He, and P. Dollár, "Focal loss for dense object detection," in *IEEE International Conference on Computer Vision*, 2017.
- [61] Q. X. Huang and L. Guibas, "Consistent shape maps via semidefinite programming," *Computer Graphics Forum*, vol. 32, no. 5, pp. 177–186, 2013.
- [62] A. Bewley, Z. Ge, L. Ott, F. Ramos, and B. Upcroft, "Simple online and realtime tracking," in *IEEE International Conference on Image Processing*, 2016.
- [63] Y. Wu, A. Kirillov, F. Massa, W.-Y. Lo, and R. Girshick, "Detectron2," <https://github.com/facebookresearch/detectron2>, 2019.
- [64] K. He, X. Zhang, S. Ren, and J. Sun, "Deep residual learning for image recognition," in *IEEE Conference on Computer Vision and Pattern Recognition*, 2016.
- [65] X. Han, Q. You, C. Wang, Z. Zhang, P. Chu, H. Hu, J. Wang, and Z. Liu, "MMPTRACK: Large-scale densely annotated multi-camera multiple people tracking benchmark," in *IEEE Winter Conference on Applications of Computer Vision*, 2023.
- [66] K. Bernardin and R. Stiefelhagen, "Evaluating multiple object tracking performance: The CLEAR MOT metrics," *EURASIP Journal on Image and Video Processing*, vol. 2008, pp. 1–10, 2008.
- [67] L. Lealtaixé, A. Milan, I. Reid, S. Roth, and K. Schindler, "MOTChallenge 2015: Towards a benchmark for multi-target tracking," in *arXiv*, 2015.
- [68] J. Luiten, A. Osep, P. Dendorfer, P. Torr, A. Geiger, L. Leal-Taixé, and B. Leibe, "HOTA: A higher order metric for evaluating multi-object tracking," *International Journal of Computer Vision*, vol. 129, no. 2, pp. 548–578, 2021.
- [69] Z. Zhong, L. Zheng, Z. Zheng, S. Li, and Y. Yang, "Camera style adaptation for person re-identification," in *IEEE Conference on Computer Vision and Pattern Recognition*, 2018.
- [70] L. Zheng, L. Shen, L. Tian, S. Wang, J. Wang, and Q. Tian, "Scalable person re-identification: A benchmark," in *IEEE International Conference on Computer Vision*, 2015.
- [71] J. Deng, W. Dong, R. Socher, L.-J. Li, K. Li, and L. Fei-Fei, "ImageNet: A large-scale hierarchical image database," in *IEEE Conference on Computer Vision and Pattern Recognition*, 2009.
- [72] G. Wang, R. Gu, Z. Liu, W. Hu, M. Song, and J.-N. Hwang, "Track without appearance: Learn box and tracklet embedding with local and global motion patterns for vehicle tracking," in *IEEE International Conference on Computer Vision*, 2021.